Materials Horizons

ROYAL SOCIETY OF CHEMISTRY

REVIEW

View Article Online
View Journal

Check for updates

Cite this: DOI: 10.1039/d4mh00313f

Porous crystalline conjugated macrocyclic materials and their energy storage applications

Yiwen Yang,† Xiaoman Yao,† Zhe Xuan, Xuanxu Chen, Yuluan Zhang, Taoping Huang, Mingjin Shi, Yifa Chen * and Ya-Qian Lan *

Received 19th March 2024,
Accepted 3rd June 2024

DOI: 10.1039/d4mh00313f

rsc.li/materials-horizons

Porous crystalline conjugated macrocyclic materials (CMMs) possess high porosity, tunable structure/function and efficient charge transport ability owing to their planar macrocyclic conjugated π-electron system, which make them promising candidates for applications in energy storage. In this review, we thoroughly summarize the timely development of porous crystalline CMMs in energy storage related fields. Specifically, we summarize and discuss their structures and properties. In addition, their energy storage applications, such as lithium ion batteries, lithium sulfur batteries, sodium ion batteries, potassium ion batteries, Li–CO_2 batteries, Li–O_2 batteries, Zn–air batteries, supercapacitors and triboelectric nanogenerators, are also discussed. Finally, we present the existing challenges and future prospects. We hope this review will inspire the development of advanced energy storage materials based on porous crystalline CMMs.

Wider impact

Porous crystalline conjugated macrocyclic materials (CMMs) with high porosity, tunable structure/function and efficient charge transport ability are promising candidates for applications in energy storage. However, few reviews have focused on a systematic summary of porous crystalline CMMs in energy storage applications. Therefore, it is meaningful to review the structures, characteristics, and applications of porous crystalline CMMs in energy storage devices in a timely and systematic manner, which could provide insightful guidance for subsequent research studies. In this review, we thoroughly summarise the timely development of porous crystalline CMMs in energy storage, discussing their current challenges and possible perspectives in this field. Beyond porous crystalline CMMs or energy storage fields, we believe that this review will also be of much interest to readers of related scientific communities, such as inorganic/organic chemistry or materials science.

School of Chemistry, South China Normal University, Guangzhou, 510006, China. E-mail: chyf927821@163.com, yqlan@m.scnu.edu.cn
† These authors contributed equally to the work.

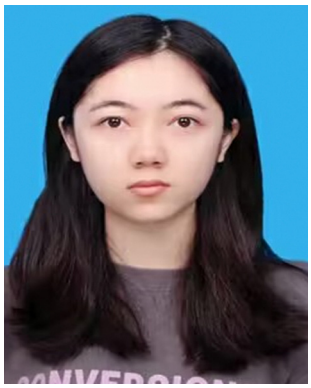

Yiwen Yang

Yiwen Yang received her BS degree at Guangdong Pharmaceutical University in 2020. She is now pursuing a postgraduate degree at South China Normal University under the supervision of Prof. Ya-Qian Lan and Prof. Yifa Chen. Her research interest focuses on the design and synthesis of porous crystalline materials for energy storage.

Xiaoman Yao

Xiaoman Yao received her BS degree at Nanjing Normal University in 2020. She is currently a PhD student in the School of Chemistry at South China Normal University, working under the supervision of Prof. Ya-Qian Lan and Prof. Yifa Chen. Her research interest focuses on the applications of porous crystalline materials in the energy-storage field.

Published on 10 June 2024. Downloaded by Zhejiang University on 6/25/2024 1:59:47 AM.

Published on 10 June 2024. Downloaded by Zhejiang University on 6/25/2024 1:59:47 AM.

1. Introduction

In nature, conjugated macrocyclic compounds, such as transition metal–nitrogen–carbon (M–N–C) compounds, have commonly existed in plants and have exhibited unique properties.[1–3] For example, consisting of four pyrrole sub-unit and methylene linkages, transition metal porphyrin (MPor) and their derivatives possess different catalytic reaction abilities, such as photosynthesis with chlorophyll, oxygen (O_2) transfer/storage or redox conversions in plants.[4,5] As an analogue of naturally existing MPor, metal phthalocyanine (MPc) can be obtained through artificial synthesis with unique photo/electrochemical properties.[6–10] In addition to MPor and MPc, other important conjugated macrocyclic compounds, such as metal phenanthroline (MPhen), have been explored.[11,12] Specifically, transition metal–nitrogen–carbon (M–N–C) compounds with specific sites such as $M–N_4$, unique electronic structures, high atom utilization efficiency, and excellent stability, are promising materials in energy storage.[13–17]

In recent years, numerous conjugated macrocyclic molecules have been utilized in energy storage fields.[18,19] Unfortunately, these molecules exhibit high solubility in electrolytes and tend to aggregate among themselves, resulting in less exposed active sites.[20] Reasonably, they are better assembled into porous frameworks to prevent these molecules from agglomeration and ensure the sufficient exposure of their active surface and porous channels that could promote charge transfer.[21–25] Therefore, the exploration of porous crystalline materials that can integrate conjugated macrocyclic molecules to meet the requirements of energy storage applications is in high demand. Porous crystalline materials, such as metal–organic frameworks (MOFs) or covalent-organic frameworks (COFs), have attracted much attention owing to their porous structures, large surface area, designable skeletons, tunable chemical functions and other characteristics.[26–29] Porous crystalline conjugated macrocyclic materials (CMMs) are a class of porous crystalline materials with conjugated macrocyclic units integrated into MOFs/COFs. Their extended π–π conjugation structures compared to other amorphous macrocyclic compounds afford them high electric conductivity, charge-transfer mobility and superior electrochemical stability that are advantageous for energy storage applications. Therefore, porous crystalline CMMs are beneficial for applications in the energy storage field because (1) the active interface and internal channels based on their porous architectures could expedite multi-electron transfer and quickly diffuse reactants and intermediates; (2) the large specific surface area provides a solid–liquid or solid–gas interface between porous crystalline CMMs and guests to facilitate fluid infiltration and rapid transfer of metal ions and further boost their performances; (3) modifiable metal sites endow rapid redox ability within their structures to meet the demand of intermediate capture or conversion in energy storage devices; (4) low density and abundant active sites can improve the energy density and coulombic efficiency of energy devices with lightweight and portability and (5) stable frameworks with high electrochemical stability endow them with high stability against acidic, basic and redox environments.

To sum up, porous crystalline CMMs have much potential in the energy storage field due to their porous frameworks, abundant active sites, designable functions, excellent electrochemical stability, efficient charge transport and intermediate conversion ability. The applications of porous crystalline CMMs in the energy storage field can be traced to 2015, in which a kind of porous crystalline CMMs was initially applied in lithium–sulfur batteries (LSBs).[30] After that, tremendous progress has been made and many works have been reported in the related energy storage field (Fig. 1).[31] Although some related reviews about porous crystalline CMMs have been reported, a systematic summary of their utilization in the energy storage field is still rare, and a comprehensive review is still needed to provide new insights for scientists.

Yifa Chen

Yifa Chen was born in 1989 in Fujian, P. R. China. He received his BS degree from the School of Chemistry, Beijing Institute of Technology. He subsequently obtained his PhD degree from the School of Chemistry and Chemical Engineering, Beijing Institute of Technology under the supervision of Prof. Bo Wang. In 2018, he became an associate professor at Nanjing Normal University (NNU, China). In 2022, he joined South China Normal University (SCNU, China) as a professor of chemistry. His research interest focuses on the fabrication of porous crystalline material-based devices, such as membranes, foams and fibers, that can be applicable in energy storage, environment treatment or photo-/electro-catalysis.

Ya-Qian Lan

Ya-Qian Lan received his BS and PhD degrees (2009) from Northeast Normal University under the supervision of Prof. Zhong-Min Su. In 2010, he joined the National Institute of Advanced Industrial Science and Technology (AIST, Japan) as a JSPS postdoctoral fellow. In 2012, he became a professor of chemistry at Nanjing Normal University (NNU, China). In 2021, he joined South China Normal University (SCNU, China) as a professor of chemistry. His current research interest focuses on the synthesis of new crystalline materials and catalytic research related to clean energy applications.

This journal is © The Royal Society of Chemistry 2024

Published on 10 June 2024. Downloaded by Zhejiang University on 6/25/2024 1:59:47 AM.

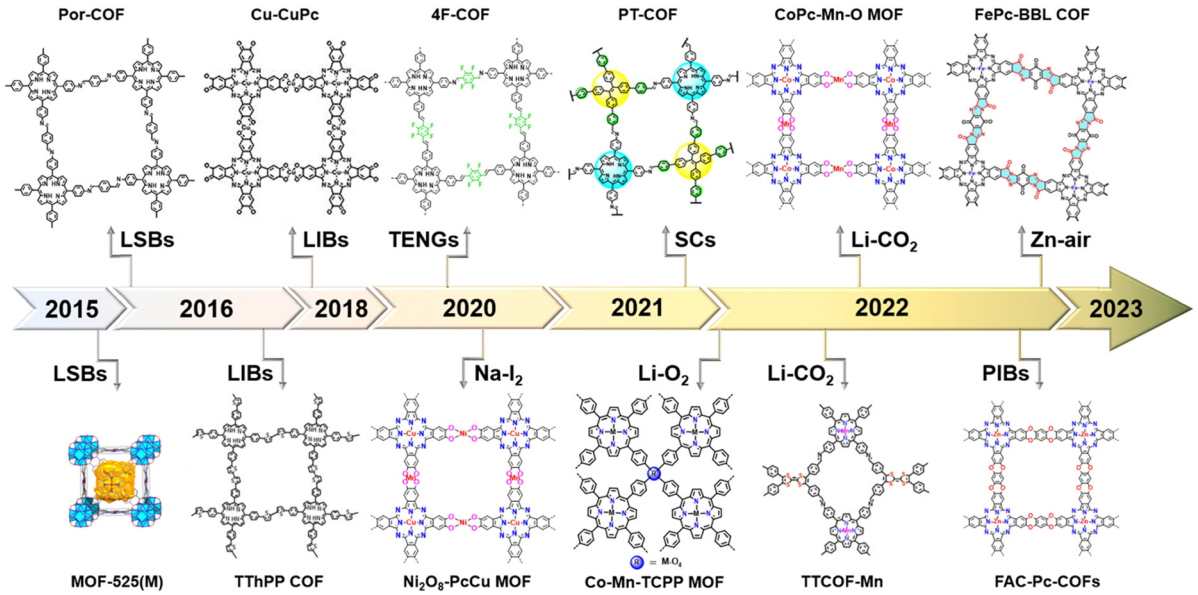

Fig. 1 Timeline of porous crystalline CMMs applied in energy storage. Image of MOF-525(M); reproduced with permission.[30] Copyright 2015, America Chemistry Society. Image of Por-COF; reproduced with permission.[32] Copyright 2016, the Royal Society of Chemistry. Image of TThPP COF; reproduced with permission.[20] Copyright 2016, America Chemistry Society. Image of Cu-CuPc; reproduced with permission.[33] Copyright 2018, Wiley-VCH. Image of 4F-COF; reproduced with permission.[34] Copyright 2020, Wiley-VCH. Image of Ni_2O_8-PcCu MOF; reproduced with permission.[35] Copyright 2020, Wiley-VCH. Image of PT-COF; reproduced with permission.[36] Copyright 2021, Wiley-VCH. Image of Co-Mn-TCPP COF; reproduced with permission.[37] Copyright 2022, Wiley-VCH. Image of TTCOF–Mn; reproduced with permission.[38] Copyright 2022, America Chemistry Society. Image of CoPc-Mn–O MOF; reproduced with permission.[39] Copyright 2022, Wiley-VCH. Image of FAC-Pc-COFs; reproduced with permission.[40] Copyright 2022, Wiley-VCH. Image of FePc-BBL COF; reproduced with permission.[41] Copyright 2022, Elsevier.

In this review, we summarize recent studies and the progress of porous crystalline CMMs in various energy storage applications (Fig. 2). Initially, we provide a brief introduction to the structural features for porous crystalline CMMs. Then, we discuss the properties of porous crystalline CMMs in energy storage, such as lithium ion batteries (LIBs), potassium ion batteries (PIBs), sodium ion batteries (SIBs), LSBs, Zn–air batteries, Li–O_2 batteries, Li–CO_2 batteries, supercapacitors (SCs) and triboelectric nanogenerators (TENGs). Finally, the perspectives and challenges for the development of porous crystalline CMMs in energy storage are also provided. This review is timely and comprehensive, and we believe that it will inspire the future development of porous crystalline CMMs in energy storage applications.

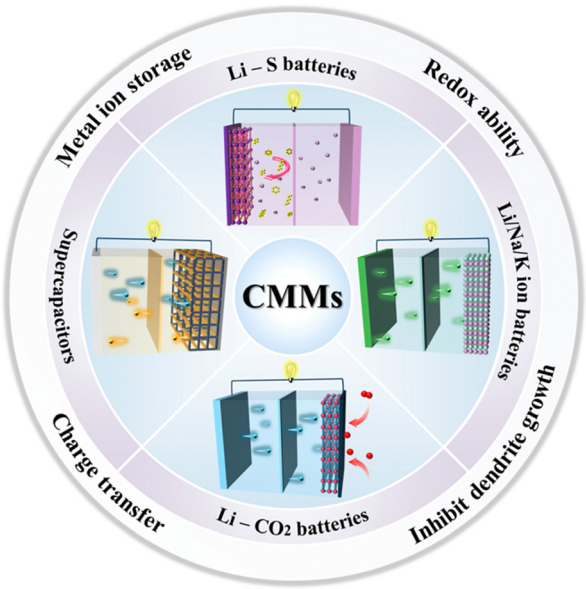

Fig. 2 Schematic illustration of porous crystalline CMMs for energy storage applications.

2. Structural features of porous crystalline CMMs

The broad applications of porous crystalline CMMs in various energy storage devices rely on the high structure tunability of porous crystalline CMMs. Based on the structural features of porous crystalline CMMs, there are basically structural features, such as functional groups, topological structures or utilization forms, that might significantly affect the applications of porous crystalline CMMs. The influence of functional groups in porous crystalline CMMs on various energy storage applications can be concluded in two aspects: (1) the functional groups on conjugated ligands for the linkage of porous crystalline CMMs and various functional groups (*i.e.*, amide, aldehyde, imide, nitro, carboxyl, cyano, sulfhydryl and hydroxyl groups) have been reported to achieve different kinds of porous crystalline CMMs through synthesis methods, such as solvothermal or ionothermal (Table 1) and (2) additional functional groups introduced by auxiliary ligands also influence the applications of porous

Published on 10 June 2024. Downloaded by Zhejiang University on 6/25/2024 1:59:47 AM.

Table 1 Summary of different linkages and ligands of porous crystalline CMMs for energy storage devices

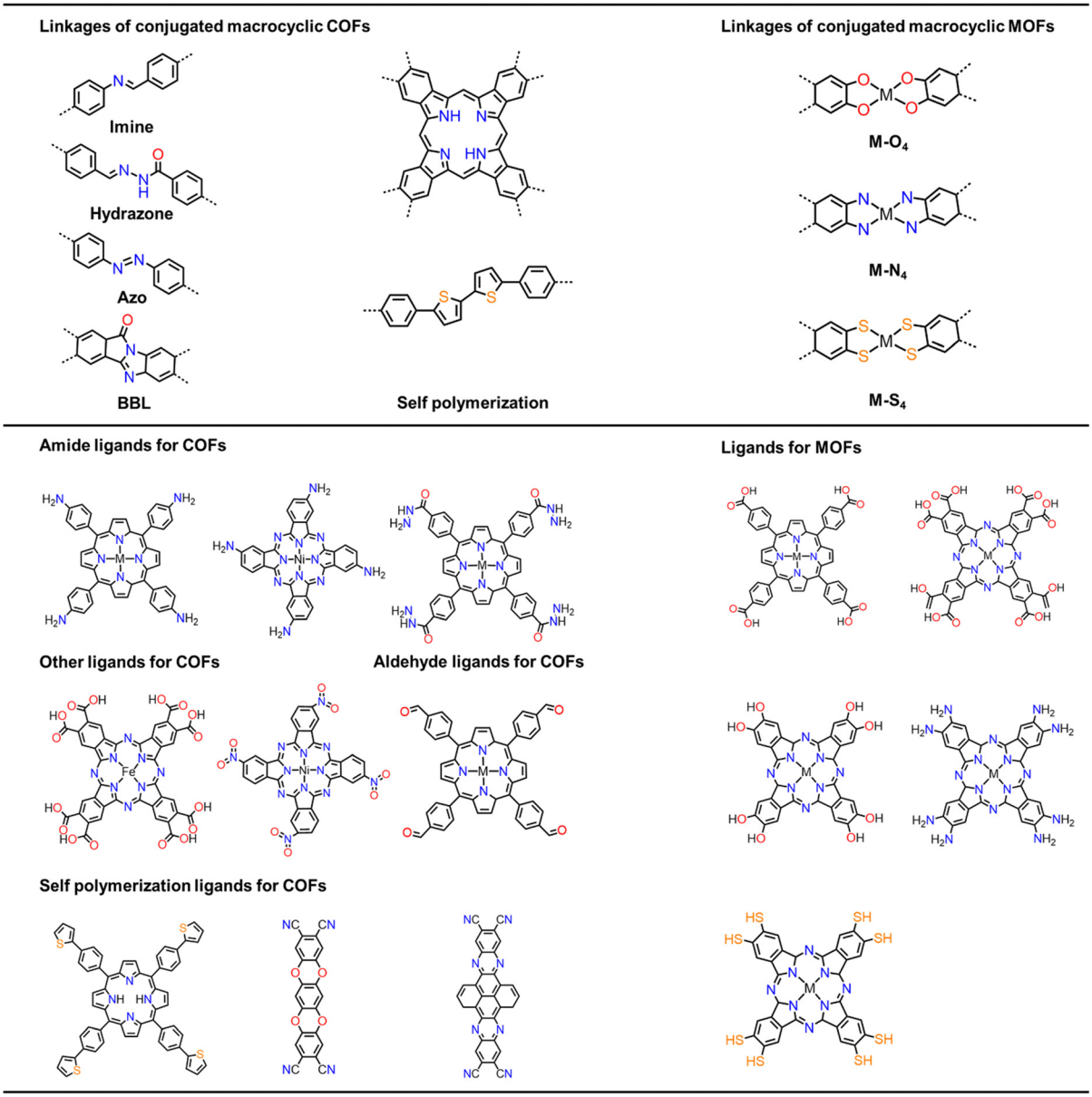

crystalline CMMs in energy storage field.[18] For example, the introduction of oxygen-rich units (*e.g.*, ether, quinone and aldehyde) is necessary to enhance the interaction with metal ions for metal ion batteries (*e.g.*, LIBs, PIBs and SIBs), thereby accelerating the diffusion kinetics of metal ions and achieving high-rate electrochemical performance.[42–46] To achieve high-energy-density LSBs, the introduction of polar units (*e.g.*, nitrile and imine groups) that are rich in sulfur and nitrogen atoms can interact with dissolved polysulfides, thereby inhibiting the shuttle effect of polysulfides and reducing the loss of active materials.[47–50] For SCs and TENGs, the existence of active sites (*e.g.*, Ni and Cu) and nitrogen-rich groups (*e.g.*, azine and imine groups) of porous crystalline CMMs is also beneficial for these applications to exhibit low resistance.[51–53] For Li–CO_2, Li–O_2 and Zn–air batteries, the charge-rich units (*e.g.*, thiazole and pyridine groups) and active metal sites (*e.g.*, Mn, Ni and Co) might accelerate the multi-electron transferred redox processes.[54–56] Therefore, the tuning of the functional groups is an essential structural feature to be considered for the applications of porous crystalline CMMs in the energy storage field.

In addition to the functional groups, topological structures are another important structural feature to be considered.[57] Through directional or post-treatment synthesis methods, porous crystalline CMMs with varied topological structures can be prepared. Based on the reported works, the tuning of topological structures mainly focuses on the pore environment (*e.g.*, pore shape, size, walls, interfaces, defects, symmetry, and spatial distribution) and hierarchical structures (*e.g.*, interpenetrating

 This journal is © The Royal Society of Chemistry 2024

Published on 10 June 2024. Downloaded by Zhejiang University on 6/25/2024 1:59:47 AM.

structures). For example, the rational design of pore sizes that can accommodate various metal ions with distinct ionic radii to facilitate the transmission of multiple metal ions (*e.g.*, Li^+, Na^+ and K^+) is significantly favourable for energy storage applications.[58] Although the regulation and control of factors beyond topological structures are still in their early stages, we believe that the complexity of the porous structures will undoubtedly broaden the exploration boundaries of porous crystalline CMMs in yet-to-be-revealed energy storage applications.

Apart from functional groups and topological structures, the utilization forms of porous crystalline CMMs can also serve as determinant factors for their applications in energy storage.[19] The utilization forms of porous crystalline CMMs in energy storage devices can be basically classified into nanomorphology (*e.g.*, nanofiber, nanosphere and nanotube) and processing forms (*e.g.*, membrane, film, fiber and monolith) that are primarily controlled by the *in situ* self-assembly or post-treatment for the application of porous crystalline CMMs in the energy storage field. For instance, in metal ion batteries (*e.g.*, LIBs, LSBs, PIB and SIBs), porous crystalline CMMs with well-tuned nanomorphology can present exposed active sites to improve the mass transfer, substrate adsorption, catalytic conversion of intermediates and rapid hopping of metal ions.[59–61] Meanwhile, advanced utilization forms, such as membrane, film, fiber or monolith, are favorable for the utilization of porous crystalline CMMs in thin and light devices with high volumetric power density (*e.g.*, SCs and TENGs).[34,36]

Thus, establishing a specific relationship between the structures and energy storage applications of porous crystalline CMMs requires multi-faceted consideration. Based on the reported works to date, porous crystalline CMMs with tunable structural features that are applied in the energy storage field can mainly be classified into conjugated macrocyclic COFs and MOFs. In the subsequent section, we discuss them elaborately and focus on the components and synthesis methodology.

2.1. Conjugated macrocyclic COFs

The development of conjugated macrocyclic COFs mainly focuses on chemically stable linkages, such as imine, hydrazine and azo linkages, as shown in Table 1. Currently, different types of conjugated macrocyclic ligands (*e.g.*, amide, aldehyde, imide, nitro and carboxyl ligands) have been reported to possess positive effects on energy storage devices. Generally, the linkages and building units of the mentioned N/O-rich ligands are beneficial for achieving targeting properties for high-performance energy storage devices.[62–64]

2.1.1. Conjugated macrocyclic amide ligands. For the synthesis of conjugated macrocyclic COFs, different conjugated macrocyclic amide ligands have been reported for potential applications in the energy storage field, such as Por- and Pc-based amide ligands. Most conjugated macrocyclic COFs applied in energy storage are synthesized by Schiff-base condensation between the amide and aldehyde groups. Based on the utilization of amide ligands, the properties of conjugated macrocyclic COFs in energy storage applications also rely on the electron withdrawing or donating groups incorporated into aldehyde ligands. For example, Lin *et al.* prepared 4F-COF through the condensation of amide-based Por and fluorine-based ligands. The 4F-COF-based TENGs exhibit an output performance of 420 V, which indicates that the electron withdrawing groups are beneficial for energy storage devices, such as TENGs, to increase surface potential.[34] Apart from electron withdrawing groups, electron donating groups can increase electron density around the metal centre of conjugated macrocyclic COFs in Li–CO_2 batteries. For instance, Zhang *et al.* combined amide-based Mn-porphyrin ligands with electron donating aldehyde ligands, such as tetrathiafulvalene (TTF), to enhance the catalytic ability of metal sites.[38] The voltage of the obtained TTCOF–Mn-based cathodes can be as low as 1.07 V at 100 mA g^{-1}.

2.1.2. Conjugated macrocyclic aldehyde ligands. Conjugated macrocyclic aldehyde ligands with the integration of M–N–C units can also be applied in the preparation of C═N linked conjugated macrocyclic COFs when combined with amide ligands. For example, Zhang *et al.* introduced redox active ligands to prepare conjugated macrocyclic COFs (TPPDA-CuPor-COF). The battery with TPPDA-CuPor-COF displays a low discharge voltage of 2.2 V.[65]

2.1.3. Conjugated macrocyclic imide ligands. Similar to amide ligands, conjugated macrocyclic imide ligands can be applied to synthesize hydrazine-linked conjugated macrocyclic COFs. Moreover, combined with aldehyde ligands possessing flexible units (*i.e.*, ester groups), they can accommodate the harsh bent conditions of all-solid-state Zn–air batteries. For example, Tang *et al.* synthesized a kind of hydrazone-connected conjugated macrocyclic COF (CoP-TOB) by condensing imide-based Por and tris-aldehydes. The CoP-TOB-based electrode maintains a superior output performance over a wide range of bent conditions (from 0° to 180°).[66]

2.1.4. Conjugated macrocyclic nitro ligands. Generally, conjugated macrocyclic nitro groups have been reported to improve the charge distribution due to their strong electron withdrawing ability.[67,68] In addition to amide and imide ligands, conjugated macrocyclic nitro ligands have also been reported for conjugated macrocyclic COFs prepared by azo condensation. Azo condensation is a simple way to prepare conjugated macrocyclic COFs that adapt to energy storage devices. For example, Zhao *et al.* designed a kind of conjugated macrocyclic COF (DAB-NiPc COF) with a 2.8 nm pore size through azo condensation of nitro-based Pc and 4,4′-diaminobiphenyln (DAB), which can be applied in LIBs with a rapid transport ability of Li^+.[58]

2.1.5. Conjugated macrocyclic carboxyl ligands. Conjugated macrocyclic double carboxyl ligands are an interesting kind of ligand for constructing ring-shaped linked conjugated macrocyclic COFs. Generally, this kind of COF possesses high mechanical stability due to its rigid and stable structure. For instance, Zhang *et al.* prepared benzoimidazobenzophenanthrolines (BBL) linked conjugated macrocyclic COFs (FePc-BBL COF) by combining double carboxylic-based Pc and aldehyde ligands that exhibit a high chemical and mechanical ability to adapt to the operating environment in Zn–air batteries.[41]

Published on 10 June 2024. Downloaded by Zhejiang University on 6/25/2024 1:59:47 AM.

2.1.6. Conjugated macrocyclic cyano ligands. In addition to direct synthesis, some ligands can be utilized for the preparation of porous crystalline CMMs achieved by self-polymerization methods. For instance, Yang *et al.* utilized an organic solvent free method (*i.e.*, ionothermal synthesis) to prepare conjugated macrocyclic COFs through self-condensation of small molecules, such as benzodioxin-2,3,9,10-tetracarbonitrile (BBTC).[40] Another self-condensation method to obtain conjugated macrocyclic COFs is *in-situ* chemical oxidation catalysed by the oxidant. For example, Yang *et al.* prepared a kind of conjugated macrocyclic COFs by the self-condensation of meso-tetrakis(4-thiophenephenyl)porhyrin (TThPP) in chloroform solution containing $FeCl_3$ under nitrogen.[20] These synthesis methods based on self-condensation will be beneficial for designing conjugated macrocyclic COFs with novel linkages.

2.2. Conjugated macrocyclic MOFs

Except for conjugated macrocyclic COFs, some representative types of ligands have been reported for the syntheses of conjugated macrocyclic MOFs, including carboxyl-based Por/Pc, hydroxyl-based Pc, double amide-based Pc and double sulfhydryl-based Pc ligands. Conjugated macrocyclic MOFs have a strong affinity to functional carriers in energy storage applications, such as Li^+, Na^+ and K^+, which endow them with good electrical conductivity and electron transfer ability to greatly facilitate the improvement of performance in energy storage applications. In addition, the coordinated metal types of conjugated macrocyclic MOFs mainly include Fe, Co, Ni, Mn, Cu, Ga and Zn (Table 1). The subsequent subsection discusses conjugated macrocyclic MOFs based on the types of ligands.

2.2.1. Conjugated macrocyclic carboxyl ligands. The types of conjugated macrocyclic carboxyl ligands applied to conjugated macrocyclic MOFs mainly include single or double carboxyl ligands. For example, Han *et al.* used tetra(4-carboxyphenyl)-porphyrin and $Co(NO_3)_2{\cdot}6H_2O$ to construct a kind of conjugated macrocyclic MOFs (Co-TCPP MOF) for anode materials of LIBs.[69] In addition, Wang *et al.* prepared a kind of conjugated macrocyclic MOFs (MOF-525(M)) that was constructed by the assembly of carboxyl-based MPor and $ZrOCl_2{\cdot}8H_2O$.[30] Stabilized by the coordination reaction between Zr^{4+} and carboxyl groups, MOF-525(M) exhibited excellent thermal and chemical stability in LSBs.

2.2.2. Conjugated macrocyclic hydroxyl ligands. Apart from the above-mentioned ligands, conjugated macrocyclic hydroxyl ligands are important ligands for constructing conjugated macrocyclic MOFs. Imparted with conjugated macrocyclic hydroxyl ligands, some transition metals, such as Mn and Co, can be integrated into the linkage of conjugated macrocyclic MOFs to prepare batteries with high energy density.[70–72] For example, Wang *et al.* prepared a kind of conjugated macrocyclic MOF (CoPc-Mn–O) by the reaction of CoPc-$(OH)_8$ and Mn[II]$(Ac)_2$. CoPc-Mn–O has dual active metal-sites, and both of them have positive effects on the performance of Li–CO_2 batteries.[39]

2.2.3. Conjugated macrocyclic amide ligands. Amide ligands are another kind of representative conjugated macrocyclic ligand for the synthesis of conjugated macrocyclic MOFs. For example, using a ball milling method, Wang *et al.* prepared a conjugated macrocyclic MOF nanosheet (Ni_2[CuPc$(NH)_8$]) with an N-rich skeleton constructed by 2,3,9,10,16,17,23,24-octaaminophthalocyaninato copper[II] and $Ni(NO_3)_2{\cdot}6H_2O$. The obtained Ni_2[CuPc$(NH)_8$] can meet the requirements of a high contact surface area and conductivity of SCs.[73]

2.2.4. Conjugated macrocyclic sulfhydryl ligands. Similarly, conjugated macrocyclic sulfhydryl ligands can also be utilized for the preparation of conjugated macrocyclic MOFs. Due to the existence of abundant M–N_4 sites that can provide extra storage sites, the obtained conjugated macrocyclic MOFs can be applied in SCs. For instance, Zhang *et al.* prepared a kind of conjugated macrocyclic MOFs (Ni_2[CuPcS_8]) by combining 2,3,9,10,16,17,23,24-octathiolphthalocyaninato copper(II) and nickel(II) acetylacetonate.[74–77] Ni_2[CuPcS_8] with Cu–N_4 linkage possesses a high electron accommodation ability that can impart SCs with highly reversible pseudocapacitive properties.

3. Applications of porous crystalline CMMs

The advantages of porous crystalline CMMs in the field of energy storage lie in unique structural features, such as conjugated macrocyclic frameworks, tunable pore structures and abundant designable functional sites, making them promising candidates in this field. Based on the above superior properties, porous crystalline CMMs have been applied in energy storage, such as LIBs, PIBs, SIBs, LSBs, Zn–air batteries, Li–O_2 batteries, Li–CO_2 batteries, SCs and TENGs. The subsequent section discusses each of them in detail, focusing on the electrochemical performance of various energy applications caused by the unique properties of porous crystalline CMMs.

3.1. LIBs

LIBs are traditional batteries that have attracted considerable attention due to their high energy density, long lifespan, lightweight, small size in a device and low pollution.[22,78–80] With porous, stable and crystalline structures, porous crystalline CMMs have gained widespread attention when utilized as battery components in LIBs. Porous crystalline CMMs adopting nanoporous structures are stable enough to ward off structural collapse caused by the insertion of Li^+. Additionally, the conjugated structure and their numerous function sites in porous crystalline CMMs reduce the possibility of dissolution in the electrolyte during cycling, making them suitable anode materials for LIBs (Table 2). For example, Sun *et al.* discovered that Por ligands in a kind of porous crystalline CMMs (PCN-600) could function as conductive substances for both electron and Li^+ transmission.[81] Concurrently, there are abundant Fe–O clusters in PCN-600 that can serve as active sites to significantly improve the specific capacity. The PCN-600-based battery exhibits a specific capacity of 1300 mA h g^{-1} at 0.4 A g^{-1} that can be attributed to the high redox activity and good carrier transport ability of porous crystalline CMM-based electrodes. Besides, another kind of porous crystalline CMMs (Cu-CuPc MOF)

 This journal is © The Royal Society of Chemistry 2024

Published on 10 June 2024. Downloaded by Zhejiang University on 6/25/2024 1:59:47 AM.

Table 2 Comparison of the electrochemical performance of various porous crystalline CMMs in LIBs

Porous crystalline CMMs	Current density (mA g^{-1})	Initial capacity (cycles per mA h g^{-1})	Cycling stability (cycles per mA h g^{-1})	Application	Ref.
PCN-600	400	~1300	300/1132	LIBs	81
TPPDA-CuPor-COF	60	137	3000/102	LIBs	66
Cu-CuPc MOF	325	128	300/650	LIBs	33
Co-TCPP MOF	100	1050	700/941	LIBs	69
NA-NiPc COF	200	437.3	700/670	LIBs	58
PPDA-NiPc COF	200	468.9	700/557	LIBs	58
DAB-NiPc COF	200	566.7	200/381	LIBs	58
TThPP COF	401	623	300/1132	LIBs	20

prepared by Nagatomi *et al.* has shown excellent performance as an anode material of LIBs (Fig. 3a).[33] The conductivity of the anode reaches up to 1.6×10^{-6} S cm^{-1} at 80 °C, which enables rapid electron/ion transfer and increases the discharge/charge rate. Besides, the improved lithium diffusion and electronic conductivity were confirmed with broad redox peaks (≈3.0 V) in the cyclic voltammogram (CV) test (Fig. 3b). The highly conjugated framework of Cu-CuPc MOF with abundant metal sites can serve as a "highway" for electronic conductivity and facilitate the lithium-ion storage kinetics of lithium anodes. Meanwhile, it has a high discharge/charge capacity (128/151 mA h g^{-1}) with superior coulombic efficiency (95%) (Fig. 3c).

In addition, the morphology, pore size, and processing form are important issues in designing porous crystalline CMMs to meet the requirements of high-performance LIBs. For the tuning of morphology, Han *et al.* prepared a kind of ultrathin lamellae-like porous crystalline CMMs (Co-TCPP MOF) for LIBs that could expose rich active sites and reduce the Li^+ diffusion distance between the contact surface and internal active site (Fig. 4b).[69] As shown in the CV spectrum (Fig. 4c), after two cycles following the formation of a solid–electrolyte-interface (SEI) film, the Co-TCPP MOF/(15 wt%)rGO electrode-based LIBs exhibit distinct anodic oxidation peaks (1.20 V) and cathodic reduction peaks (0.42 V) along with overlapping large integral areas. The excellent specific capacity and reversibility of the LIBs can be attributed to the high lithium-ion storage ability of the Co-TCPP MOF. Moreover, a specific capacity of 1050 mA h g^{-1} can be obtained for the Co-TCPP MOF/(15 wt%) rGO-based electrode at 100 mA g^{-1} (Fig. 4d). In addition, a large pore size can provide extra storage space, which makes it easy

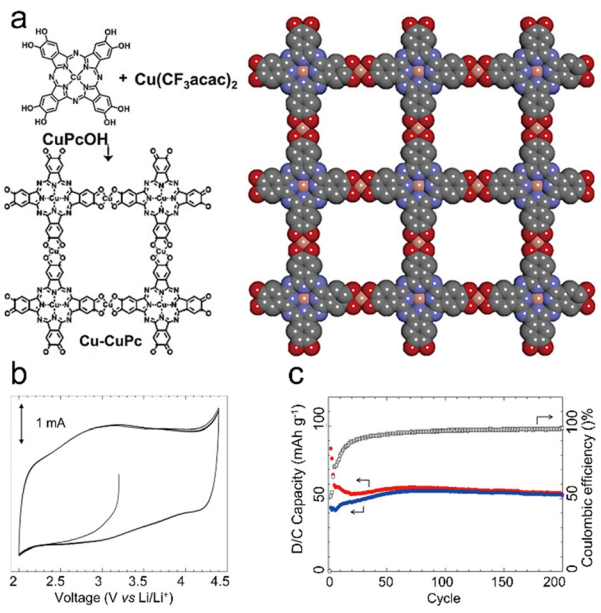

Fig. 3 (a) Synthesis and structure of Cu-CuPc. (b) Cyclic voltage spectrum of Cu-CuPc. (c) Cycling performance of LIBs with Cu-CuPc at 0.4C (red: charge capacity, blue: discharge capacity, and square: coulombic efficiency). Reproduced with permission.[33] Copyright 2018, Wiley-VCH.

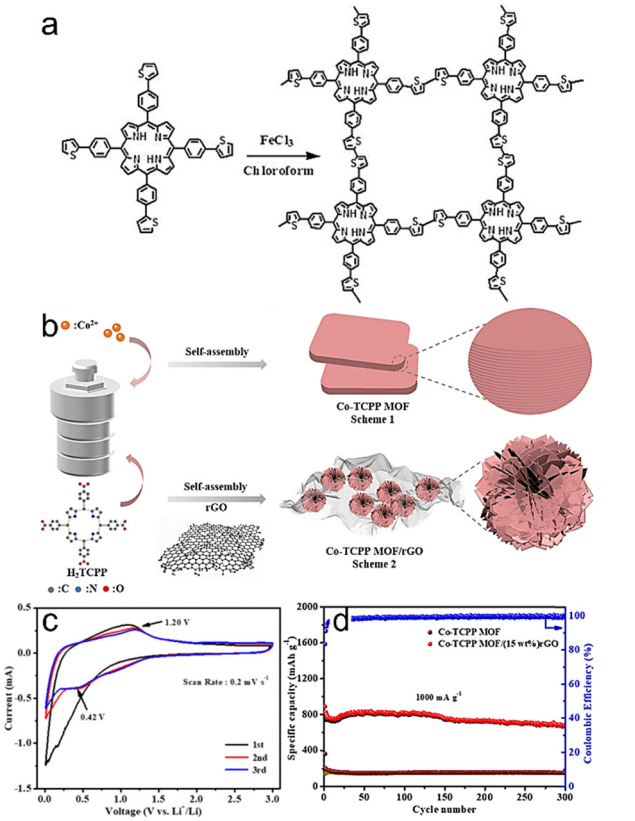

Fig. 4 (a) Synthesis and structure of TThPP. Reproduced with permission.[20] Copyright 2016, American Chemical Society. (b) Synthesis procedure of the Co-TCPP MOF and Co-TCPP MOF/rGO composites. (c) Cyclic voltage spectrum of Co-TCPP MOF/(15 wt%) rGO at 0.2 mV s^{-1}. (d) Long-term cycling performance of Co-TCPP MOF/(15 wt%) rGO electrode at 1 A g^{-1}. Reproduced with permission.[69] Copyright 2021, Elsevier.

Published on 10 June 2024. Downloaded by Zhejiang University on 6/25/2024 1:59:47 AM.

for electrolyte ions to enter and leave, thus increasing the electrode capacity. For instance, Zhao *et al.* synthesized COFs with three kinds of pore sizes (*i.e.*, 1.5, 2.2 and 2.8 nm). After 700 cycles, the capacity of the DAB-NiPc COF (2.8 nm)-based electrode is maintained at 941 mA h g^{-1}. In contrast, the capacities of NA-NiPc COF (1.5 nm) and PPDA-NiPc COF (2.2 nm)-based electrodes are 557 and 670 mA h g^{-1}, respectively. This could be ascribed to the suitable pore size and stable π–π conjugate construction beneficial for the rapid Li^+ transfer process.[58] Except for morphology and pore size, the processing form is also an important issue to be considered for porous crystalline CMMs in the application of LIBs. For example, Yang *et al.* fabricated a kind of porous crystalline CMMs (TThPP COF) film-based anode materials for LIBs, which could provide abundant channels and short-end paths for Li^+ intercalation and prolapse (Fig. 4a). The battery with TThPP COF shows a specific capacity of 666 mA h g^{-1} at 0.2 A mg^{-1} with a coulombic efficiency of 99.3% after 200 cycles.[20]

3.2. Other metal ion batteries

3.2.1. SIBs. SIBs, with the advantage of widely available sodium and similar chemistry to LIBs, hold promise for energy storage.[82–86] However, the large ionic radius of Na^+ leads to the collapse of the electrode structure after rapid intercalation/deintercalation, which limits its application in SIBs. Therefore, it is necessary to explore new electrode materials to take advantage of SIBs. As a kind of electrode material with a porous structure and controllable pore size, porous crystalline CMMs could allow multiple Na^+ to rapidly transport, which allows them to be potentially applied in SIBs. For instance, Yang *et al.* synthesized a kind of porous crystalline CMMs (MPc-2D-cCOFs) applied as the electrode material in SIBs. The battery with the MPc-2D-cCOF electrode exhibits excellent Na^+ storage ability in SIBs.[87] At 50 and 1000 mA g^{-1}, the electrode presents reversible capacities of 538 and 342 mA h g^{-1}, respectively, showing good electrochemical performance. Except for SIBs, porous crystalline CMMs can also be applied in Na–I_2 batteries to prevent the polyiodide from dissoluting.[35] For example, Wang *et al.* demonstrated that a kind of porous crystalline CMMs (Fe_2–O_8-PcCu) could effectively prevent the polyiodide from dissolution in Na–I_2 batteries (Fig. 5a).[65,84,88,89] Fe_2–O_8-PcCu-based electrode achieves strong adsorption of polyiodide due to the existence of functional metal sites. In addition, it exhibits moderate specific capacity (208 mA h g^{-1}) and cycle stability (3200 cycles at 1.5 A g^{-1}) in Na–I_2 batteries (Fig. 5b and c). These results prove the important role of porous crystalline CMMs as battery components for SIBs.

3.2.2. PIBs. As an alternative to LIBs, PIBs possess lower redox potential and higher energy density.[90–94] However, the large ionic radius of K^+ leads to a high volume change during discharging/charging, resulting in lower battery performance. In general, traditional commercial graphite is commonly applied in PIBs, but it is easy to collapse after intercalation/deintercalation of K^+. To discover novel electrode materials to replace graphite, Yang *et al.* prepared a kind of porous crystalline CMMs (QPP-FAC-Pc-COF) using a solvent-free, simple, and rapid method (Fig. 6a). QPP-FAC-Pc-COF displays outstanding electrical conductivity (1.94 × 10^{-4} S cm^{-1}); meanwhile, its stable and porous N/O-rich backbone can afford huge volume change during discharging/charging, which exhibits remarkable performance in K^+ storage.[40] A high specific capacity (424 mA h g^{-1}) can be achieved by QPP-FAC-Pc-COF at 0.5 A g^{-1} after 100 cycles. Additionally, the capacity maintains nearly 100%

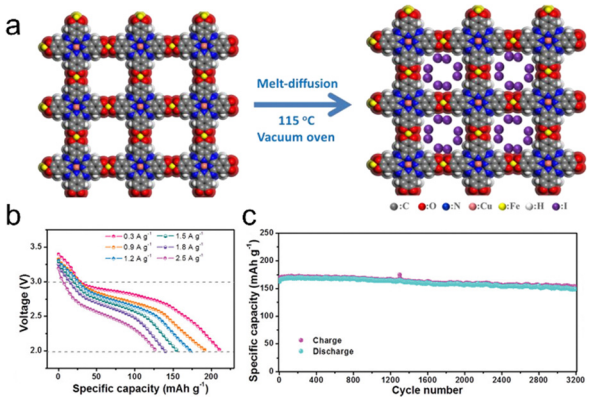

Fig. 5 (a) Schematic illustration of PcCu-MOF/I_2 composites obtained using a melt-diffusion method. (b) Galvanostatic discharge voltage profiles of the Fe_2–O_8-PcCu/I_2 electrode at different current densities. (c) Long-term cycling performance of the Fe_2–O_8-PcCu/I_2 electrodes at 1.5 A g^{-1}. Reproduced with permission.[35] Copyright 2020, Wiley-VCH.

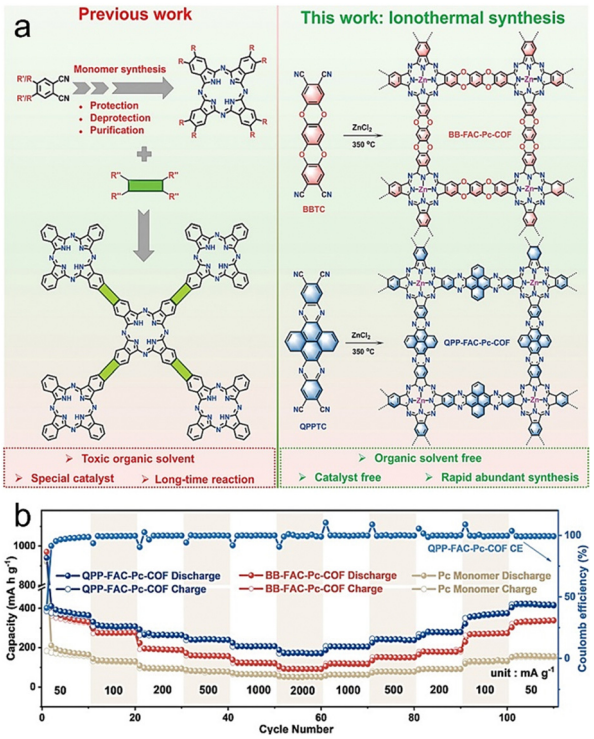

Fig. 6 (a) Comparison of synthesis methods between previous works and this work for the construction of FAC-Pc-COFs. (b) Rate performance of FAC-Pc-COFs and Pc monomer. Reproduced with permission.[40] Copyright 2022, Wiley-VCH.

This journal is © The Royal Society of Chemistry 2024

Published on 10 June 2024. Downloaded by Zhejiang University on 6/25/2024 1:59:47 AM.

over 10 000 cycles at 2 A g^{-1}, which indicates its excellent cycling stability (Fig. 6b).

3.3. Li–CO_2 batteries

Owing to the high energy density and wide application prospects, the Li–CO_2 batteries are regarded as a new and promising energy storage technology.[78,79,94,95] Nevertheless, Li–CO_2 batteries present several challenges; the notorious one is the insulation of the discharge product (Li_2CO_3). Porous crystalline CMMs are ideal platforms for the construction of functional catalysts because their active metal sites can catalyze the discharge/charge processes (Fig. 7a). For instance, the TTCOF–Mn-based cathode synthesized by Zhang *et al.* is beneficial for the processes of CO_2 reduction reaction (CRR). It can achieve an overpotential of 1.7 V at 100 mA g^{-1} and is stable enough to obtain a 2.6 V terminal discharge potential after 180 cycles at 300 mA g^{-1} (Fig. 7c–e).[38] These results indicate that the functional Mn–N_4 unit of TTCOF–Mn can contribute to the adsorption of CO_2 molecules and promote the four-electron aprotic CO_2 conversion process (Fig. 7b). Another example of porous crystalline CMMs (Cu-TCPP COF) prepared by Xu *et al.* can also be applied in Li–CO_2 batteries.[80] Specifically, the battery with Cu-TCPP COF displays a remarkable specific capacity (20.39 Ah g^{-1}) at 0.1 A g^{-1} and can be operated for 123 cycles at 0.5 A g^{-1}. In addition, a low overpotential of 1.8 V can be detected at 2 A g^{-1}. The high performance of the Cu-TCPP COF-based cathode can be attributed to the charge-rich Cu–N_4 functional sites in the Cu-TCPP COF that could enhance the rapid kinetics of CRR.

To reduce the polarization of Li_2CO_3, some advanced techniques, such as light-assist technology, have been applied in Li–CO_2 batteries.[96–98] Coupling with light is an effective way to significantly reduce the polarization of Li_2CO_3, which can regulate the separation efficiency of photo-generated electrons and holes participating in battery reactions to design high-performance Li–CO_2 batteries. For instance, CoPc-Mn–O synthesized by Wang *et al.* presented high photocatalytic effects owing to its high photo-absorption ability, efficient separation and transmission of charges/holes as well as redox ability.[39] CoPc-Mn–O-based electrodes can provide a 0.05 V overpotential and up to 98.5% round-trip efficiency under full spectrum conditions. In addition, the battery can be rapidly discharged/charged for 60 h at 0.02 mA cm^{-2}. These results imply that the introduction of conjugated light-absorbing groups in porous crystalline CMMs will be a promising approach for developing light-assisted Li–CO_2 batteries with high output performance and low polarity.

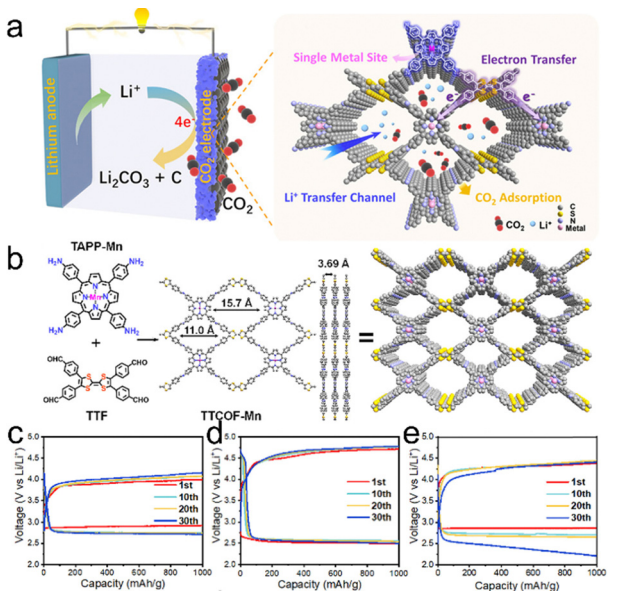

Fig. 7 (a) Schematic illustration of the advantages of the TTCOF-M based Li–CO_2 battery. (b) The synthesis and structure of TTCOF–Mn. Discharge/charge curves of different COF based cathode catalysts at 0.1 A g^{-1}: (c) TTCOF–Mn, (d) TTCOF-2H, and (e) COF-366-Mn. Reproduced with permission.[38] Copyright 2022, American Chemical Society.

3.4. Li–O_2 batteries

Compared to LIBs, Li–O_2 batteries with higher theoretical specific energy (3500 Wh kg^{-1}) hold much promise in rechargeable batteries yet still face several challenges, such as polarization, high overpotential, low capacity retention and poor cycling performance, due to the limited kinetically redox reactions.[99–103] To address these issues, Nam *et al.* explored an epitaxial growth strategy to achieve the modification of Co–Mn-TCPP on MXene ($Ti_3C_2T_x$) to prepare electrode materials (CMT@MXene) of Li–O_2 batteries (Fig. 8a).[37] Co–Mn-TCPP is a kind of porous crystalline CMM with a porous organic skeleton imparted with two kinds of metal ions in different valence states (Fig. 8b). With a specific capacity of 1000 mA h g^{-1}, the CMT@MXene-based Li–O_2 batteries could be cycled for 247 cycles at 500 mA g^{-1} (Fig. 8c and d). Therefore, the performance of Li–O_2 batteries can be improved by adjusting the energy band gap and the position of the energy band edge in porous crystalline CMMs. Apart from Co/Mn-coordinated Por, Ni-coordinated Por has also been used in the design of Li–O_2 batteries.[104] To improve the conductivity of the material, Ren *et al.* integrated the π-conjugated electronic structure of Ni-bis(dithienyl) and Co-coordinated Por into porous crystalline CMMs, resulting in Ni-TAPP-Co with a conductivity as high as 1.18×10^{-4} S m^{-1}. Furthermore, Ni-TAPP-Co-based Li–O_2 batteries display a remarkable discharge capacity (17 104 mA h g^{-1}) at 500 mA g^{-1}, which confirms that the introduced active metal and π-conjugated units are effective in improving the conductivity and ORR/OER catalytic activity of Li–O_2 batteries.

3.5. LSBs

Owing to their high theoretical energy density (2600 Wh kg^{-1}), LSBs have attracted much attention around the world,[25,105–108] yet their insufficient recycling performances caused by the shuttling of polysulfides have limited their commercialization processes. To date, porous crystalline CMMs have been reported as sulfur hosts, separators and sulfur conducting additives for LSBs (Table 3).[25] For a sulfur host, Liao *et al.* successfully prepared a kind of efficient and stable porous crystalline CMMs (Por-COF) with appropriate pores that can

Published on 10 June 2024. Downloaded by Zhejiang University on 6/25/2024 1:59:47 AM.

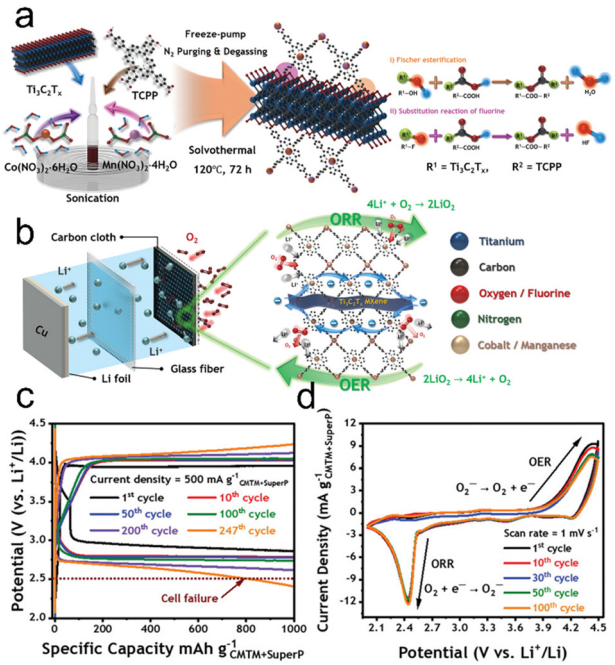

Fig. 8 (a) Schematic diagram of the formation process of CMT@MXene. (b) Schematic illustration of the advantages of the CMT@MXene electrocatalyst for Li–O_2 batteries. (c) Terminal potentials of the charge–discharge curves at 1000 mA h $g^{-1}_{CMTM+SuperP}$, tested at 500 mA $g^{-1}_{CMTM+SuperP}$. (d) CV curves at a scan rate of 1 mV s^{-1}. Reproduced with permission.[37] Copyright 2022, Wiley-VCH.

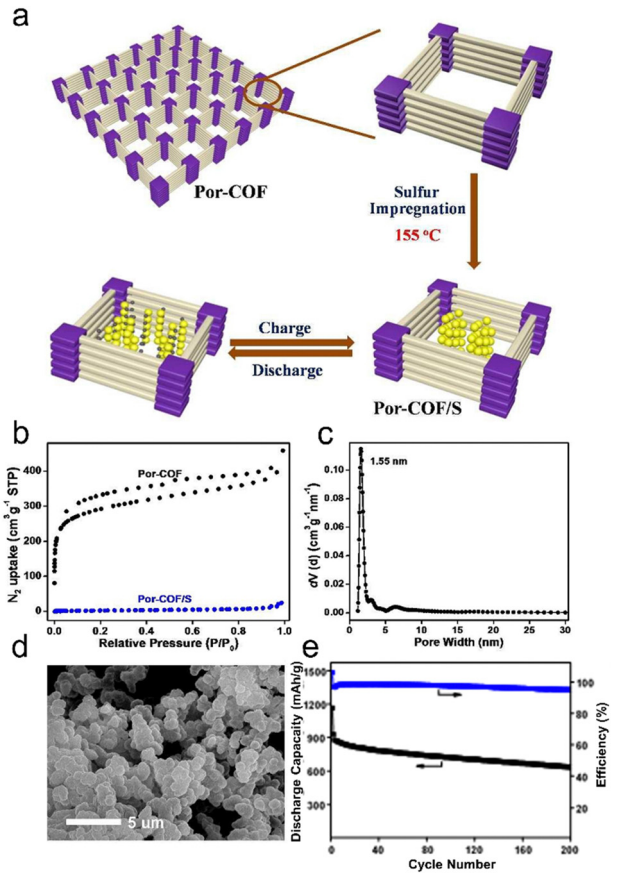

Fig. 9 (a) Schematic diagram of the synthesis of Por-COFs and the discharge/charge processes of LSBs with Por-COFs. (b) N_2 sorption results of Por-COF and Por-COF/S composites. (c) Pore size distribution of Por-COFs. (d) SEM image of the Por-COF/S composite. (e) Cycling performance of the Por-COF/S composite at 0.5C. Reproduced with permission.[32] Copyright 2016, the Royal Society of Chemistry.

be applied to the sulfur host (Fig. 9a–d).[32] After 200 cycles, the Por-COF-based electrode presents a 633 mA h g^{-1} capacity and maintains a low capacity decay rate (only 0.16% per cycle) at a discharge/charge rate of 0.5C (Fig. 9e). In addition, Hu *et al.* synthesized a kind of layered porous crystalline CMMs (COF-MF) with a microflower superstructure (Fig. 10a and b).[109] The COF-MF-based cathode could be fully recycled at a high sulfur loading of 4.1 mg cm^{-2}. After recycling for 150 cycles, the capacity retention rate is up to 80.3% at 3.43 mA cm^{-2}, demonstrating the excellent catalytic ability of COF-MF for redox processes (Fig. 10c). Similarly, MOF-525(Cu) prepared by Wang *et al.* was also utilized as host materials for sulfur.[30] MOF-525(Cu)-based electrode displays a capacity of 700 mA h g^{-1} at 0.5C after 200 cycles.

In addition to host materials, porous crystalline CMMs can also be applied for sulfur conducting additive of LSBs. To be applied as a sulfur conducting additive, the pore environment, conductivity and electrochemical stability of porous crystalline CMMs need to be considered. For instance, Kiraly *et al.* prepared GaTCPP(Ni) by doping Ni^{2+} in GaTCPP MOFs. Modified with Ni^{2+}, GaTCPP(Ni)-based LSBs display relatively low interphase contact resistance both before (4.6 Ω) and after (0.6 Ω) cycling.[110] At 0.2C, a discharge capacity of 778 mA h g^{-1} can be achieved by the GaTCPP(Ni)-based electrode after 50 cycles, which is higher than the original GaTCPP electrode. These results demonstrate that GaTCPP(Ni) with abundant Ni^{2+} active sites, porous structure, high conductivity and excellent electrochemical stability is very beneficial in increasing the electrode capacity.

For the separator, Hu *et al.* decorated a kind of porous crystalline CMMs (Co-PCN-222) on CNTs by applying an *in situ*

Table 3 Comparison of the electrochemical performance of various porous crystalline CMMs in LSBs

Porous crystalline CMMs	Current density (C)	Initial capacity (cycles per mA h g^{-1})	Cycling stability (cycles per mA h g^{-1})	Application	Ref.
Por-COF	0.5	1166	200/633	LSBs	32
COF-MF	0.5	898	300/467	LSBs	109
MOF-525(Cu)	0.5	~1000	200/700	LSBs	30
GaTCPP(Ni)	0.5	609.9	200/478.9	LSBs	110
Co-PCN-222	0.5	900	150/735	LSBs	111
Hf-CoDPBP/CNT	2	~1000	500/513	LSBs	112

This journal is © The Royal Society of Chemistry 2024

Published on 10 June 2024. Downloaded by Zhejiang University on 6/25/2024 1:59:47 AM.

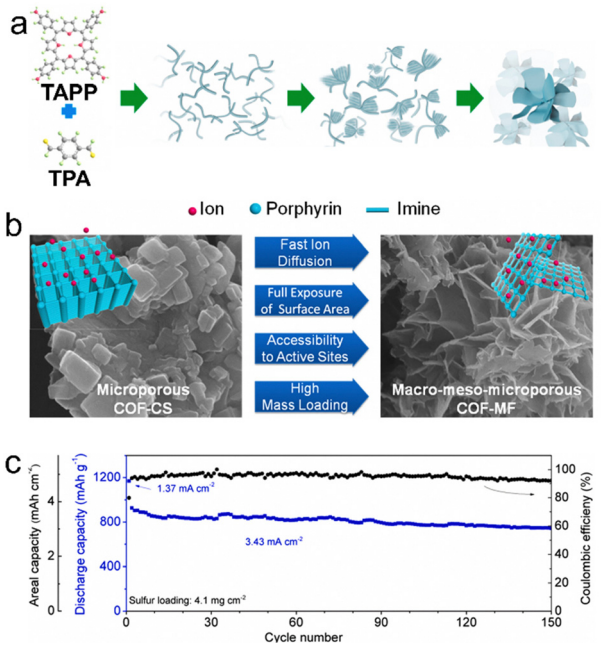

Fig. 10 (a) Proposed mechanism for the COF-MF formation. (b) SEM images and structural features of COF-MF and COF-CS. (c) Cycling performance of COF-MF@S at a high sulfur loading of 4.1 mg cm^{-2}. Reproduced with permission.[109] Copyright 2019, Elsevier.

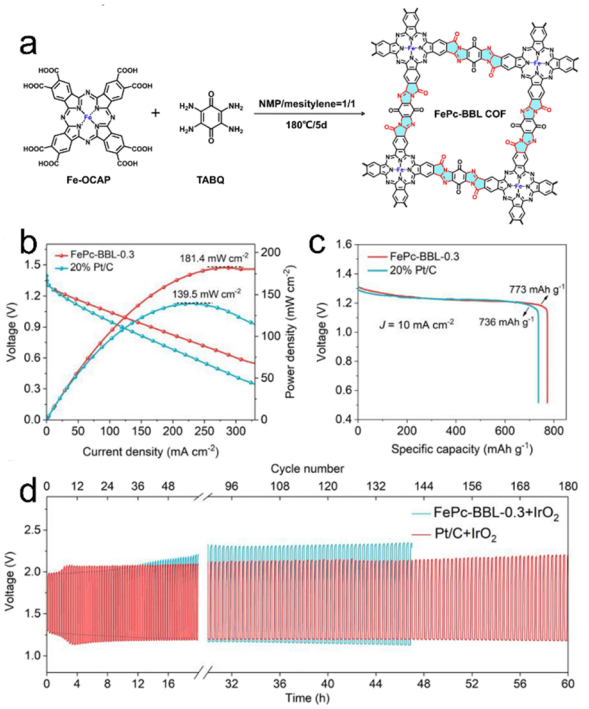

Fig. 11 (a) Schematic diagram of the synthesis and structure of FePc-BBL COFs. (b) Discharge polarization and power density plots. (c) Typical specific capacity curves at 10 mA cm^{-2}. (d) Galvanostatic discharge/charge cycle performance at 5 mA cm^{-2}. Reproduced with permission.[41] Copyright 2022, Elsevier.

method to obtain a hybrid material (PCN@CNT).[111] With a PCN@CNT coated separator, the battery shows specific capacities of 1157 mA h g^{-1} at 0.1C and 696 mA h g^{-1} at 2C in the LSBs. In addition, a 0.067% capacity decay rate is detected after 500 cycles at 1C, demonstrating that abundant Co–N_4 and Zr^{4+} sites of porous crystalline CMMs can act as active centers for the adsorption and conversion of polysulfides. Different from the above-mentioned examples, Ren *et al.* modified a kind of porous crystalline CMMs (Hf-CoDPBP) onto CNTs by applying the post-synthesis method and obtained a kind of hybrid material (Hf-CoDPBP/CNT) that could selectively inhibit the shuttling of polysulfides.[112] At an operating current density of 0.1C, the electrode with Hf-CoDPBP/CNT coated separator presents high initial specific capacity (1325 mA h g^{-1}) and moderate capacity retention after 500 cycles (513 mA h g^{-1}) at 2C, which can be attributed to the synergistic effects between active Co–N_4 sites and hybrid structures after modifying with CNTs.

3.6. Zn–air batteries

Zn–air batteries, possessing environmental friendliness, low cost and high energy density, are attractive technologies for future energy storage.[113–116] To achieve efficient energy conversion, highly active and durable oxygen reduction reaction (ORR) or oxygen evolution reaction (OER) electrocatalysts need to be designed. Porous crystalline CMMs can serve as promising non-precious metal electrocatalysts for the ORR that can promote multi-electron oxygen reactions at low overpotential. In addition, they are important platforms that can integrate functional catalytic units into porous frameworks to design electrocatalysts for Zn–air batteries with excellent performance. For example, Zhang *et al.* reported a kind of porous crystalline CMM (FePc-BBL COF) with BBL linkage (Fig. 11a). The FePc-BBL COF with the advantages of novel stepped-type BBL linkage, porous structure and highly active Fe–N_4 site shows high ORR activity, maximum power density (181.4 mW cm^{-2}), specific capacity (773 mA h g^{-1}) and long-term durability when used as cathode electrocatalyst in Zn–air batteries (Fig. 11b–d).[41] In addition to traditional Zn–air batteries, porous crystalline CMMs also show good electrocatalytic performance and stability in flexible all-solid Zn–air batteries. For instance, Tang *et al.* introduced a trialdehyde linker into porous crystalline CMMs by applying a liquid-gas interface strategy to produce CoP-TOB films.[67] CoP-TOB films can be utilized as air electrodes to facilitate the electrocatalytic processes of ORR and OER. Notably, the discharge/charge voltage gap is 0.88 V, and the battery shows high stability under bending conditions from 0° to 180° at 1 mA cm^{-2}. To date, although porous crystalline CMMs with different active sites have been applied in improving the ORR/OER kinetics of Zn–air batteries, it still needs to pay attention to the three-phase interface among the electrolyte environment, zinc oxides and air to reveal the complicated interaction mechanisms.

3.7. SCs

With the advantages of high power density and long lifetime, SCs are suitable for applications where large amounts of current can be delivered shortly.[117–120] In general, the performances of SCs depend on the characteristics of electrode

Published on 10 June 2024. Downloaded by Zhejiang University on 6/25/2024 1:59:47 AM.

material, such as conductivity, surface area, porosity, and structural periodicity. In previously reported works, the integration of conjugated macrocyclic units enhanced the conductivity of porous crystalline CMMs. For example, Patra *et al.* prepared a kind of porous crystalline CMMs (PT-COF) with Por units.[36] PT-COF shows a conductivity (σ) of 7.06×10^{-8} S cm^{-1} at room temperature. In addition, at 1 A g^{-1}, a specific capacitance of 1443 F g^{-1} can be achieved and high-capacity retention (91%) can be retained after 3000 cycles.

Moreover, some porous crystalline CMMs applied for SCs are reported in nanosheet forms that could offer accessible active sites and large surface areas, providing abundant reaction and adsorption sites to enhance the application properties of porous crystalline CMMs.[73] For example, Zhao *et al.* synthesized a kind of porous crystalline CMM (MPF) nanosheet using a facile solvothermal method. Then, MXene/MPF films as flexible supercapacitor electrodes can be fabricated by embedding MPF nanosheets in highly conductive two-dimensional ultrathin materials (MXene) through direct hydrogen bonding interactions.[121] The synergistic effect between the MPF nanosheet and MXene enables MXene/MPF films to exhibit excellent capacitance properties under different test conditions. Notably, the battery displays 326.1 F g^{-1}, 1.64 F cm^{-2}, and 694.2 F cm^{-3} at 0.1 A g^{-1}, 1 mA cm^{-2} and 1 mA cm^{-3}, respectively. Moreover, a capacitance retention of 95.9% is maintained after 7000 cycles. In the applications of SCs, porous crystalline CMM-based nanosheets can also be prepared by applying the ball-milling method. For instance, Wang *et al.* successfully synthesized a kind of porous crystalline CMMs ($Ni_2[CuPc(NH)_8]$) and fabricated them into nanosheets by applying a ball-milling method (Fig. 12a).[73] With high electrical conductivity, porosity, and crystallinity properties (Fig. 12b), the nanosheets exhibit p-type semiconductor behavior at room temperature. Specifically, it has an 18.9 mF cm^{-2} surface capacitance with an excellent mobility of about 1.5 cm^2 V^{-1} s^{-1} (Fig. 12c and d). Except for the ball-milling method, the surfactant-assisted synthesis method is another effective means of producing porous crystalline CMM nanosheets. For instance, Cao *et al.* successfully applied polyvinylpyrrolidone (PVP) as the surfactant molecule to prepare 2D PPF-3 nanosheet-based SCs.[122] It has been proved that the material has high capacity, superior rate capability and long-term cycling stability. At 1.5 A g^{-1}, it displays a specific capacitance of 360.1 F g^{-1}. Moreover, a specific capacity retention of 56.8% can be achieved at 30.0 A g^{-1}.

Compared with traditional SCs, non-aqueous electrolyte-based SCs can run with operating voltage windows of up to 3 V and extent temperature ranges (−30 to 70 °C) that can meet the requirements of SCs with high output power.[124,125] For instance, Zhang *et al.* prepared a $Ni_2[CuPc(NH)_8]$ MOF that could act as electrodes of quasi-solid symmetric SCs when combined with gelatin/Na_2SO_4 gel electrolyte.[123] The experimental results show that this battery has a high power density (32.1 kW kg^{-1}) and energy density (51.6 Wh kg^{-1}). Apart from electrodes, porous crystalline CMMs can also be utilized as solid electrolytes for SCs. For instance, Zhang *et al.* prepared a

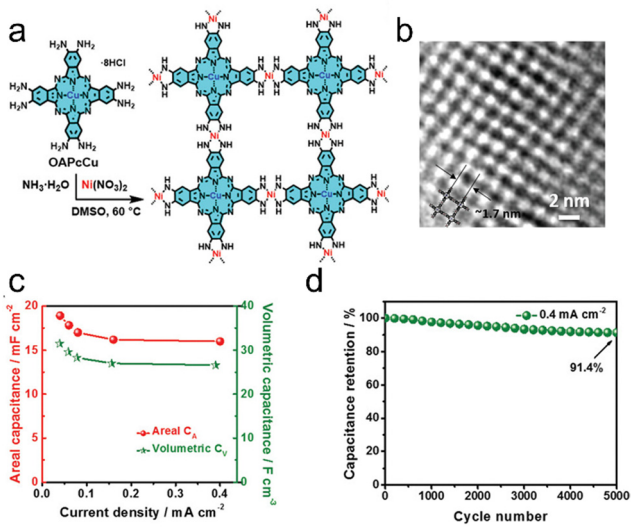

Fig. 12 (a) Schematic diagram of the synthesis and structure of $Ni_2[CuPc(NH)_8]$. (b) HRTEM image of $Ni_2[CuPc(NH)_8]$ nanosheets. (c) Specific capacitances calculated from GCD curves as a function of current density. (d) Long-term cycling performance at 0.4 mA cm^{-2} under voltage window of 0.8 V. Reproduced with permission.[123] Copyright 2020, Wiley-VCH.

kind of porous crystalline CMMs ($Ni_2[CuPcS_8]$) as an electrolyte for all-solid SCs. $Ni_2[CuPcS_8]$-based SCs exhibit superior capacitive properties with a 2.3 V operating voltage and a 57.4 Wh kg^{-1} energy density.[74] These results are significant for the development of high-performance capacitive electrode materials for SCs. Based on the above-mentioned results, the highly π-conjugated extended structures and active metal centers of porous crystalline CMMs enable SCs to balance conductivity and capacitance performance. With the emergence of novel SC components (*e.g.*, solid-state electrolytes, flexible electrodes and multicomponent electrodes), it is necessary to develop new strategies, such as introducing flexible ligands for developing advanced utilization forms (*e.g.*, fiber, film or membrane) of porous crystalline CMMs in SCs.

3.8. TENGs

TENGs are devices that use the energy generated by friction to drive the operation of a nanogenerator.[34,126–130] When two materials are rubbed against each other, a separation of electrostatic charges occurs, resulting in an electric potential difference. Using this electrostatic effect, electrical energy can be obtained by utilizing frictional energy through TENGs. The output power of TENGs is proportional to the square of frictional charge density. Therefore, the charge density of the friction surface is closely associated with the corresponding performance of the TENGs. For instance, Lin *et al.* synthesized a series of porous crystalline CMMs (*i.e.*, CH_3COF, H-COF, 2F-COF, and 4F-COF) with different functional groups (*i.e.*, methyl, hydrogen, and fluorine) applied as triboelectric pairs in TENGs (Fig. 13a).[34] The results show that a 420 V output open circuit voltage of 4F-COF-based TENGs can be achieved at a 64 μA short-circuit current, which is better than that of 2F-COF (383 V), H-COF (330 V) and CH_3COF (248 V). In addition, the

This journal is © The Royal Society of Chemistry 2024

Published on 10 June 2024. Downloaded by Zhejiang University on 6/25/2024 1:59:47 AM.

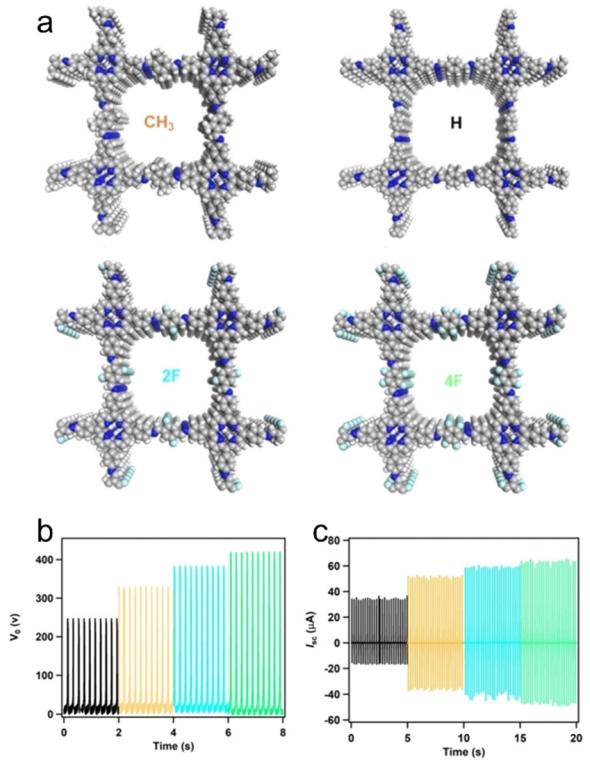

Fig. 13 (a) Structures of of CH_3-COF, H-COF, 2F-COF and 4F-COF. Comparison of the output performance of TENGs with different COFs (black: H-COF, orange: CH_3-COF, cyan: 2F-COF, and green: 4F-COF). (b) Open-circuit voltage (V_o) and (c) short-circuit current (I_{sc}). Reproduced with permission.[34] Copyright 2020, Wiley-VCH.

4F-COF-based TENG exhibits a 2858 mW m^{-2} power density (Fig. 13b and c). The superior performance of the 4F-COF-based TENGs can be attributed to the high electron affinity of the fluorinated groups in the 4F-COF. The results verify that the highly tunable structures and functions of porous crystalline CMMs make them potential electrode materials for TENGs. Therefore, the introduction of organic ligands with special electron withdrawing/donating ability is crucial for the preparation of TENGs based on porous crystalline CMMs with high triboelectric properties.

4. Perspectives

Based on the above-mentioned results, the contribution of porous crystalline CMMs in the energy storage field can be basically summarized as follows. The presence of tunable pore structures of porous crystalline CMMs is suitable for reversible metal-ion storage and diffusion. Meanwhile, they exhibit high chemical stability and good tolerance for volume changes caused by charging or discharging. Besides, compared with the other reported materials, porous crystalline CMMs are superior in catalysis during the processes of discharging/charging to promote the redox reaction kinetics. However, the applications of porous crystalline CMMs in energy storage still face severe challenges: (1) synthesis issues: the structure rigidity of conjugated units makes them to be relatively hard in the preparation of porous crystalline CMMs to obtain a structure with high crystallinity; (2) stability issue: the coordinated metal center of macrocyclic molecular would face leaching problems under strong acidic or alkaline conditions; (3) dilemma between electrical conductivity and crystallinity: there is a balance between the crystalline structure and electrical conductivity; (4) high cost: complicated and relatively stringent synthesis processes of conjugated macrocyclic ligands limit their large-scale production and (5) lack in utilization forms: most of them are based on powder forms and only limited processing examples have been reported.[38]

Although porous crystalline CMMs have witnessed rapid development as competitive candidates applied in energy storage in the past decades, a huge scope of improvement is yet to be explored in the structures and utilization forms of porous crystalline CMMs. For metal-ion batteries, there is a balance between the crystalline structure and electrical conductivity for high-rate metal-ion batteries, and it needs to rationally design porous crystalline CMMs with specific construction struts to achieve both metal-ion storage ability and high electrical conductivity.[131–135] For Li–CO_2, Li–O_2 and Zn–air batteries, integrating various metal sites with functional groups to adjust the energy bandgap can broaden the electrochemical window for related redox reactions (*e.g.*, CRR, CER, ORR and OER),[136–140] yet their underlying mechanisms of the synergistic interactions among different functional units in enhancing the catalytic activity of specific redox reactions still need to be explored. For SCs and TENGs, the applications of porous crystalline CMMs require more advanced utilization forms (*e.g.*, fiber, membrane and film) to be fitted into frequent folding environments or special application conditions.[141–144]

Based on the advantages and challenges, we propose some perspectives for porous crystalline CMMs: (1) for the synthesis issue, the exploration of green and sustainable media with high solubility for macrocyclic ligands, such as ionic liquid or supercritical CO_2 (SC CO_2), might be needed; (2) for the stability issue, the design of more stable conjugated macrocyclic MOFs (*i.e.*, zirconium-based, aluminum-based and titanium-based MOFs) and stronger bonding modes (*i.e.*, oxazole, hydrazone, sp^3 and sp^2 linkage) for COFs as well as hybridization with other protection materials are desired; (3) for the dilemma between electrical conductivity and crystallinity, well-tuned nanomorphology (*i.e.*, nanosheet, nanofiber and nanotube) of porous crystalline CMMs would meet the requirements; (4) for the high cost and large-scale production of conjugated macrocyclic ligands, green and cheap synthetic techniques or one-pot synthetic strategies from the precursors (*i.e.*, Por, Pc, Phen) of ligand to porous crystalline CMMs are necessary, and (5) for the lack of utilization forms, advanced applicable forms such as membrane, film, fiber, foam and monolith would be demanded for specific scenery of different energy storage applications.

5. Conclusions

In summary, this review summarizes the significant progress of porous crystalline CMMs for various energy storage applications.

Published on 10 June 2024. Downloaded by Zhejiang University on 6/25/2024 1:59:47 AM.

Initially, the structures of porous crystalline CMMs are discussed in detail. After that, we review different applications of porous crystalline CMMs in the energy storage field. Finally, their current challenges and possible perspectives in energy storage applications are presented. We hope this review will inspire more interest in scientists applying porous crystalline CMMs for advanced applications in energy storage.

Conflicts of interest

There are no conflicts to declare.

Acknowledgements

This work was financially supported by the National Key R&D Program of China (2023YFA1507204). National Natural Science Foundation of China (Grants 22171139, 22225109, 22071109). Natural Science Foundation of Guangdong Province (No. 2023B1515020076).

Notes and references

1 M. O. Senge, N. N. Sergeeva and K. J. Hale, *Chem. Soc. Rev.*, 2021, **50**, 4730–4789.
2 S. Hiroto, Y. Miyake and H. Shinokubo, *Chem. Rev.*, 2017, **117**, 2910–3043.
3 W. Zhang, W. Lai and R. Cao, *Chem. Rev.*, 2017, **117**, 3717–3797.
4 T. Xiu, L. Liu, S. Liu, H. Shehzad, Y. Liang, M. Zhang, G. Ye, C. Jiao, L. Yuan and W. Shi, *J. Hazard. Mater.*, 2024, **465**, 133508.
5 Y. Liu, Y. Kang, M. Bao, H. Cao, C. Weng, X. Dong, H. Hao, X. Tang, J. Chen, L. Wang and C. Xu, *J. Hazard. Mater.*, 2024, **462**, 132756.
6 S. Huang, K. Chen and T.-T. Li, *Coord. Chem. Rev.*, 2022, **464**, 214563.
7 W. Ji, T.-X. Wang, X. Ding, S. Lei and B.-H. Han, *Coord. Chem. Rev.*, 2021, **439**, 213875.
8 H. Dai, J. Dong, M. Wu, Q. Hu, D. Wang, L. Zuin, N. Chen, C. Lai, G. Zhang and S. Sun, *Angew. Chem., Int. Ed.*, 2021, **60**, 19852–19859.
9 L. Li, X. Tang, S. Huang, C. Lu, D. Lützenkirchen-Hecht, K. Yuan, X. Zhuang and Y. Chen, *Angew. Chem., Int. Ed.*, 2023, **62**, e202301642.
10 N. Lv, Q. Li, H. Zhu, S. Mu, X. Luo, X. Ren, X. Liu, S. Li, C. Cheng and T. Ma, *Adv. Sci.*, 2023, **10**, 2206239.
11 S. Yang, Y. Yu, X. Gao, Z. Zhang and F. Wang, *Chem. Soc. Rev.*, 2021, **50**, 12985–13011.
12 Ö. Bekaroğlu, *Functional Phthalocyanine Molecular Materials*, Springer, 2010.
13 H. Wang, Q. Wu, L. Cheng, L. Chen, M. Li and G. Zhu, *Energy Storage Mater.*, 2022, **52**, 495–513.
14 S. Okada and J. Yamaki, *J. Electrochem. Soc.*, 1989, **136**, 2437.
15 M. Arakawa, J. Yamaki and T. Okada, *J. Electrochem. Soc.*, 1984, **131**, 2605.
16 J. Yamaki and A. Yamaji, *J. Electrochem. Soc.*, 1982, **129**, 5.
17 S. J. Thompson, M. R. Brennan, S. Y. Lee and G. Dong, *Chem. Soc. Rev.*, 2018, **47**, 929–981.
18 B. Y. Zhang, W. B. Wang, L. N. Liang, Z. C. Xu, X. Y. Li and S. L. Qiao, *Coord. Chem. Rev.*, 2021, **436**, 213782.
19 D. Y. Wang, R. L. Liu, W. Guo, G. Li and Y. Z. Fu, *Coord. Chem. Rev.*, 2021, **429**, 213650.
20 H. Yang, S. L. Zhang, L. H. Han, Z. Zhang, Z. Xue, J. Gao, Y. J. Li, C. S. Huang, Y. P. Yi, H. B. Liu and Y. L. Li, *ACS Appl. Mater. Interfaces*, 2016, **8**, 5366–5375.
21 Y. Zang, D.-Q. Lu and Y.-Q. Lan, *Sci. Bull.*, 2022, **67**, 1621–1624.
22 L. Chen, K. Ding, K. Li, Z. Li, X. Zhang, Q. Zheng, Y.-P. Cai and Y.-Q. Lan, *EnergyChem*, 2022, **4**, 100073.
23 Y. Zhang, C. Guo, L. Zhou, X. Yao, Y. Yang, H. Zhuang, Y.-R. Wang, Q. Huang, Y. Chen, S.-L. Li and Y.-Q. Lan, *Small Sci.*, 2023, **3**, 2300056.
24 C. Guo, J. Zhou, Y. Chen, H. Zhuang, Q. Li, J. Li, X. Tian, Y. Zhang, X. Yao, Y. Chen, S.-L. Li and Y.-Q. Lan, *Angew. Chem., Int. Ed.*, 2022, **134**, e202210871.
25 Y. Zhang, C. Guo, J. Zhou, X. Yao, J. Li, H. Zhuang, Y. Chen, Y. Chen, S.-L. Li and Y.-Q. Lan, *Small*, 2023, **19**, 2206616.
26 M. Wang, M. Ballabio, M. Wang, H.-H. Lin, B. P. Biswal, X. Han, S. Paasch, E. Brunner, P. Liu, M. Chen, M. Bonn, T. Heine, S. Zhou, E. Cánovas, R. Dong and X. Feng, *J. Am. Chem. Soc.*, 2019, **141**, 16810–16816.
27 Y. Yue, P. Cai, X. Xu, H. Li, H. Chen, H. Zhou and N. Huang, *Angew. Chem., Int. Ed.*, 2021, **60**, 10806–10813.
28 Y. Yue, P. Cai, K. Xu, H. Li, H. Chen, H.-C. Zhou and N. Huang, *J. Am. Chem. Soc.*, 2021, **143**, 18052–18060.
29 B. Li, S. Zhang, L. Kong, H. Peng and Q. Zhang, *Adv. Mater.*, 2018, **30**, 1870160.
30 Z. Q. Wang, B. X. Wang, Y. Yang, Y. J. Cui, Z. Y. Wang, B. L. Chen and G. D. Qian, *ACS Appl. Mater. Interfaces*, 2015, **7**, 20999–21004.
31 L. S. Peng, L. Shang, T. R. Zhang and G. I. N. Waterhouse, *Adv. Energy Mater.*, 2020, **10**, 2003018.
32 H. Liao, H. Wang, H. Ding, X. Meng, H. Xu, B. Wang, X. Ai and C. Wang, *J. Mater. Chem. A*, 2016, **4**, 7416.
33 H. Nagatomi, N. Yanai, T. Yamada, K. Shiraishi and N. Kimizuka, *Chem. – Eur. J.*, 2018, **24**, 1806–1810.
34 C. Lin, L. Sun, X. Meng, X. Yuan, C.-X. Cui, H. Qiao, P. Chen, S. Cui, L. Zhai and L. Mi, *Angew. Chem., Int. Ed.*, 2022, **61**, e202211601.
35 F. X. Wang, Z. C. Liu, C. Q. Yang, H. X. Zhong, G. Nam, P. P. Zhang, R. H. Dong, Y. P. Wu, J. Cho, J. Zhang and X. L. Feng, *Adv. Mater.*, 2020, **32**, 1905361.
36 B. C. Patra and S. Bhattacharya, *Chem. Mater.*, 2021, **33**, 8512–8523.
37 S. Nam, M. Mahato, K. Matthews, R. W. Lord, Y. Lee, P. Thangasamy, C. W. Ahn, Y. Gogotsi and I. K. Oh, *Adv. Funct. Mater.*, 2023, **33**, 2210702.
38 Y. Zhang, R. L. Zhong, M. Lu, J. H. Wang, C. Jiang, G. K. Gao, L. Z. Dong, Y. F. Chen, S. L. Li and Y. Q. Lan, *ACS Cent. Sci.*, 2021, **7**, 175–182.

 This journal is © The Royal Society of Chemistry 2024

Published on 10 June 2024. Downloaded by Zhejiang University on 6/25/2024 1:59:47 AM.

39 J.-H. Wang, S. Li, Y. Chen, L.-Z. Dong, M. Liu, J.-W. Shi, S.-L. Li and Y.-Q. Lan, *Adv. Funct. Mater.*, 2022, **32**, 2210259.
40 X. Y. Yang, L. Gong, K. Wang, S. H. Ma, W. P. Liu, B. W. Li, N. Li, H. H. Pan, X. Chen, H. L. Wang, J. M. Liu and J. Z. Jiang, *Adv. Mater.*, 2022, **34**, 2207245.
41 Z. Zhang, W. Wang, X. Wang, L. Zhang, C. Cheng and X. Liu, *Chem. Eng. J.*, 2022, **435**, 133872.
42 T. Shimizu, K. Wakamatsu, Y. Yamada, Y. Toyoda, S. Akine, K. Yoza and H. Yoshikawa, *ACS Appl. Mater. Interfaces*, 2021, **13**, 40612–40617.
43 J. Chen, J. Guo, T. Zhang, C. Wang, N. Ding, Q. Zhang, H. Yang, X. Liu, D. Li, Z. Li, S. Zhong and S. Wang, *RSC Adv.*, 2016, **6**, 52850–52853.
44 K. Li, J. Zhu, Z. Xu, Q. Liu, S. Zhai, N. Wang, X. Wang and Z. Li, *ACS Appl. Mater. Interfaces*, 2021, **13**, 30583–30593.
45 N. A. Kumar, R. R. Gaddam, M. Suresh, S. R. Varanasi, D. Yang, S. K. Bhatia and X. S. Zhao, *J. Mater. Chem. A*, 2017, **5**, 13204–13211.
46 H.-G. Wang, H. Wang, Y. Li, Y. Wang and Z. Si, *J. Energy Chem.*, 2021, **58**, 9–16.
47 W. Huang, Z. Lin, H. Liu, R. Na, J. Tian and Z. Shan, *J. Mater. Chem. A*, 2018, **6**, 17132–17141.
48 X.-X. Yang, X.-T. Li, C.-F. Zhao, Z.-H. Fu, Q.-S. Zhang and C. Hu, *ACS Appl. Mater. Interfaces*, 2020, **12**, 32752–32763.
49 J. Kim, H. Shin, D.-J. Yoo, S. Kang, S.-Y. Chung, K. Char and J. W. Choi, *Adv. Funct. Mater.*, 2021, **31**, 2106679.
50 S. Zhou, S. Yang, X. Ding, Y. Lai, H. Nie, Y. Zhang, D. Chan, H. Duan, S. Huang and Z. Yang, *ACS Nano*, 2020, **14**, 7538–7551.
51 W. Wang, H. Xu, W. Zhao, J. Zhao, M. Jiang, S. Liu, W. Huang and Q. Zhao, *Chem. Eng. J.*, 2022, **428**, 131089.
52 D. Das and S. Kurungot, *Energy Technol.*, 2020, **8**, 2000061.
53 C. Zhang, S. Duan, M. Zhou, Z. Liu, H. Ren, S. Sasaki and X.-F. Wang, *Chem. Eng. J.*, 2022, **450**, 138000.
54 H.-S. Kim, B. Kim, H. Park, J. Kim and W.-H. Ryu, *Adv. Energy Mater.*, 2022, **12**, 2103527.
55 B. Kim, K. Shin, G. Henkelman and W.-H. Ryu, *Chem. Eng. J.*, 2023, **477**, 147141.
56 K. Cui, Q. Wang, Z. Bian, G. Wang and Y. Xu, *Adv. Energy Mater.*, 2021, **11**, 2102062.
57 Z. Li, T. He, Y. Gong and D. Jiang, *Acc. Chem. Res.*, 2020, **53**, 1672–1685.
58 J. Zhao, M. Zhou, J. Chen, L. Tao, Q. Zhang, Z. Li, S. Zhong, H. Fu, H. Wang and L. Wu, *Chem. Eng. J.*, 2021, **425**, 131630.
59 X. Zhang, G. Zhu, M. Wang, J. Li, T. Lu and L. Pan, *Carbon*, 2017, **116**, 686–694.
60 X. Yang, B. Dong, H. Zhang, R. Ge, Y. Gao and H. Zhang, *RSC Adv.*, 2015, **5**, 86137–86143.
61 Z. A. Ghazi, L. Zhu, H. Wang, A. Naeem, A. M. Khattak, B. Liang, N. A. Khan, Z. Wei, L. Li and Z. Tang, *Adv. Enegry Mater.*, 2016, **6**, 1601250.
62 Y. Cao, H. Fang, C. Guo, W. Sun, Y. Xu, Y. Wu and Y. Wang, *Angew. Chem., Int. Ed.*, 2023, **62**, e202302143.
63 S. Karak, K. Dey and R. Banerjee, *Adv. Mater.*, 2022, **34**, 2202751.
64 Y. Ge, J. Li, Y. Meng and D. Xiao, *Nano Energy*, 2023, **109**, 108297.
65 C. Guo, B. Han, W. Sun, Y. Cao, Y. Zhang and Y. Wang, *Angew. Chem., Int. Ed.*, 2022, **61**, e202213276.
66 L. Gong, X. Y. Yang, Y. Gao, G. X. Yang, Z. H. Yu, X. Z. Fu, Y. H. Wang, D. D. Qi, Y. Z. Bian, K. Wang and J. Z. Jiang, *J. Mater. Chem. A*, 2022, **10**, 16595–16601.
67 J. Tang, Z. Liang, H. Qin, X. Liu, B. Zhai, Z. Su, Q. Liu, H. Lei, K. Liu, C. Zhao, R. Cao and Y. Fang, *Angew. Chem., Int. Ed.*, 2023, **135**, e202214449.
68 M. Wang, J. Duan, X. Yang, Y. Wang, Y. Duan and Q. Tang, *Nano Energy*, 2020, **73**, 104747.
69 Y. Han, Z. J. Liu, F. F. Zheng, Y. X. Bai, Z. Q. Zhang, X. G. Li, W. W. Xiong, J. H. Zhang and A. H. Yuan, *J. Alloys Compd.*, 2021, **881**, 160531.
70 Y. Mao, C. Tang, Z. Tang, J. Xie, Z. Chen, J. Tu, G. Cao and X. Zhao, *Energy Storage Mater.*, 2019, **18**, 405–413.
71 S. Li, Y. Liu, J. Zhou, S. Hong, Y. Dong, J. Wang, X. Gao, P. Qi, Y. Han and B. Wang, *Energy Environ. Sci.*, 2019, **12**, 1046–1054.
72 W. Ma, S. Lu, X. Lei, X. Liu and Y. Ding, *J. Mater. Chem. A*, 2018, **6**, 20829–20835.
73 M. C. Wang, H. H. Shi, P. P. Zhang, Z. Q. Liao, M. Wang, H. X. Zhong, F. Schwotzer, A. S. Nia, E. Zschech, S. Q. Zhou, S. Kaskel, R. H. Dong and X. L. Feng, *Adv. Funct. Mater.*, 2020, **30**, 2002664.
74 P. Zhang, M. Wang, Y. Liu, Y. Fu, M. Gao, G. Wang, F. Wang, Z. Wang, G. Chen, S. Yang, Y. Liu, R. Dong, M. Yu, X. Lu and X. Feng, *J. Am. Chem. Soc.*, 2023, **145**, 6247–6256.
75 Z. Li, S. Wang, J. Shi, Y. Liu, S. Zheng, H. Zou, Y. Chen, W. Kuang, K. Ding, L. Chen, Y. Lan, Y. Cai and Q. Zheng, *Energy Storage Mater.*, 2022, **47**, 262–270.
76 T. Wei, J. Lu, M. Wang, C. Sun, Q. Zhang, S. Wang, Y. Zhou, D. Chen and Y. Lan, *Chin. J. Chem.*, 2023, **41**, 1861–1874.
77 F.-C. Shen, C. Guo, S.-N. Sun, Z. Lei and Y.-Q. Lan, *Inorg. Chem.*, 2022, **61**, 11182–11188.
78 B. Lu, Z. Min, X. Xiao, B. Wang, B. Chen, G. Lu, Y. Liu, R. Mao, Y. Song, X.-X. Zeng, Y. Sun, J. Yang and G. Zhou, *Adv. Mater.*, 2024, **36**, 2309264.
79 J. Zou, G. Liang, F. Zhang, S. Zhang, K. Davey and Z. Guo, *Adv. Mater.*, 2023, **35**, 2210671.
80 Y. Y. Xu, H. Gong, H. Ren, X. L. Fan, P. Li, T. F. Zhang, K. Chang, T. Wang and J. P. He, *Small*, 2022, **18**, 2203917.
81 L. Sun, J. Xie, Z. D. Chen, J. Wu and L. Li, *Dalton Trans.*, 2018, **47**, 9989–9993.
82 X. Wang, Q. Zhang, C. Zhao, H. Li, B. Zhang, G. Zeng, Y. Tang, Z. Huang, I. Hwang, H. Zhang, S. Zhou, Y. Qiu, Y. Xiao, J. Cabana, C.-J. Sun, K. Amine, Y. Sun, Q. Wang, G.-L. Xu, L. Gu, Y. Qiao and S.-G. Sun, *Nat. Energy*, 2024, **9**, 184–196.
83 Q. Wang, D. Zhou, C. Zhao, J. Wang, H. Guo, L. Wang, Z. Yao, D. Wong, G. Schuck, X. Bai, J. Lu and M. Wagemaker, *Nat. Sustainable*, 2024, **7**, 338–347.
84 Z. Wang, S. Chen, J. Qiu, J. Li, W. Zhao, Y. Ji, X. Yao, Z. Chen, K. Li, M. Dong, F. Pan and L. Yang, *Adv. Energy Mater.*, 2023, **13**, 2302514.

Published on 10 June 2024. Downloaded by Zhejiang University on 6/25/2024 1:59:47 AM.

85 Z. Bai, Q. Yao, M. Wang, W. Meng, S. Dou, H. K. Liu and N. Wang, *Adv. Energy Mater.*, 2024, 2303788.
86 Y. Lin, Q. Peng, L. Chen, Q. Zuo, Q. Long, F. Lu, S. Huang, Y. Chen and Y. Meng, *Energy Storage Mater.*, 2024, **67**, 103211.
87 X. Yang, Y. Jin, B. Yu, L. Gong, W. Liu, X. Liu, X. Chen, K. Wang and J. Jiang, *Sci. China Chem.*, 2022, **65**, 1291–1298.
88 L. Xiang, S. Yuan, F. Wang, Z. Xu, X. Li, F. Tian, L. Wu, W. Yu and Y. Mai, *J. Am. Chem. Soc.*, 2022, **144**, 15497–15508.
89 H. Tian, H. Shao, Y. Chen, X. Fang, P. Xiong, B. Sun, P. H. L. Notten and G. Wang, *Nano Energy*, 2019, **57**, 692–702.
90 J. C. Pramudita, D. Sehrawat, D. Goonetilleke and N. Sharma, *Adv. Energy Mater.*, 2017, **7**, 1602911.
91 M. Xia, H. Fu, K. Lin, A. M. Rao, L. Cha, H. Liu, J. Zhou, C. Wang and B. Lu, *Energy Environ. Sci.*, 2024, **17**, 1255–1265.
92 S. Dhir, S. Wheeler, I. Capone and M. Pasta, *Chem*, 2020, **6**, 2442–2460.
93 X. Wu, S. Qiu, Y. Liu, Y. Xu, Z. Jian, J. Yang, X. Ji and J. Liu, *Adv. Mater.*, 2022, **34**, 2106876.
94 Q. Deng, Y. Yang, K. Yin, J. Yi, Y. Zhou and Y. Zhang, *Adv. Energy Mater.*, 2023, **13**, 2302398.
95 J. Chen, X.-Y. Chen, Y. Liu, Y. Qiao, S.-Y. Guan, L. Li and S.-L. Chou, *Energy Environ. Sci.*, 2023, **16**, 792–829.
96 L. Long, Y. Ding, N. Liang, J. Liu, F. Liu, S. Huang and Y. Meng, *Small*, 2023, **19**, 2300519.
97 Y.-H. Liu, J. Qu, W. Chang, C.-Y. Yang, H.-J. Liu, X.-Z. Zhai, Y. Kang, Y.-G. Guo and Z.-Z. Yu, *Energy Storage Mater.*, 2022, **50**, 334–343.
98 J. Li, X. Du, X. Wang, X. Yuan, D. Guan and J. Xu, *Angew. Chem., Int. Ed.*, 2024, e202319211.
99 N. Feng, P. He and H. Zhou, *Adv. Energy Mater.*, 2016, **6**, 1502303.
100 Q. Xiong, C. Li, Z. Li, Y. Liang, J. Li, J. Yan, G. Huang and X. Zhang, *Adv. Mater.*, 2022, **34**, 2110416.
101 Z. Peng, *Nat. Chem.*, 2023, **15**, 1206–1208.
102 H.-D. Lim, B. Lee, Y. Bae, H. Park, Y. Ko, H. Kim, J. Kim and K. Kang, *Chem. Soc. Rev.*, 2017, **46**, 2873–2888.
103 J. Park, S. H. Lee, H. Jung, D. Aurbach and Y. Sun, *Adv. Mater.*, 2018, **30**, 1704162.
104 S.-W. Ke, W. Li, Y. Gu, J. Su, Y. Liu, S. Yuan, J.-L. Zuo, J. Ma and P. He, *Sci. Adv.*, 2023, **9**, eadf2398.
105 C. Guo, M. Liu, G. Gao, X. Tian, J. Zhou, L. Dong, Q. Li, Y. Chen, S. Li and Y. Lan, *Angew. Chem., Int. Ed.*, 2022, **134**, e202113315.
106 Z. Zhu, Y. Zeng, Z. Pei, D. Luan, X. Wang and X. W. (David) Lou, *Angew. Chem., Int. Ed.*, 2023, **135**, e202305828.
107 X. Yao, C. Guo, C. Song, M. Lu, Y. Zhang, J. Zhou, H. M. Ding, Y. Chen, S.-L. Li and Y. Q. Lan, *Adv. Mater.*, 2023, **35**, 2208846.
108 G.-K. Gao, Y.-R. Wang, S.-B. Wang, R.-X. Yang, Y. Chen, Y. Zhang, C. Jiang, M.-J. Wei, H. Ma and Y.-Q. Lan, *Angew. Chem., Int. Ed.*, 2021, **133**, 10235–10242.
109 X. Hu, J. Jian, Z. Fang, L. Zhong, Z. Yuan, M. Yang, S. Ren, Q. Zhang, X. Chen and D. Yu, *Energy Storage Mater.*, 2019, **22**, 40–47.
110 N. Kiraly, D. Capkova, M. Almasi, T. Kazda, O. Cech, P. Cudek, A. S. Fedorkova, M. Lisnichuk, V. Meynen and V. Zelenak, *RSC Adv.*, 2022, **12**, 23989–24002.
111 X. H. Hu, T. Huang, S. P. Wang, S. J. Lin, Z. H. Feng, L. H. Chung and J. He, *Electrochim. Acta*, 2021, **398**, 139317.
112 Y. Ren, M. Y. Wang, X. Y. Yang, W. J. Xu, Q. J. Lei, J. Zhang, J. X. Wen, J. X. Gu, Z. S. Chao and H. G. Jin, *Chem. Eng. J.*, 2022, **437**, 135150.
113 T. Jin, J. Nie, M. Dong, B. Chen, J. Nie and G. Ma, *Nano-Micro Lett.*, 2022, **15**, 26.
114 Z. Chen, X. Peng, Z. Chen, T. Li, R. Zou, G. Shi, Y. Huang, P. Cui, J. Yu, Y. Chen, X. Chi, K. P. Loh, Z. Liu, X. Li, L. Zhong and J. Lu, *Adv. Mater.*, 2023, 2209948.
115 T. Zhou, N. Zhang, C. Wu and Y. Xie, *Energy Environ. Sci.*, 2020, **13**, 1132–1153.
116 Q. Hu, G. Li, G. Li, X. Liu, B. Zhu, X. Chai, Q. Zhang, J. Liu and C. He, *Adv. Energy Mater.*, 2019, **9**, 1970045.
117 Q. Zhu, D. Zhao, M. Cheng, J. Zhou, K. A. Owusu, L. Mai and Y. Yu, *Adv. Energy Mater.*, 2019, **9**, 1901081.
118 L. Zhang, D. Shi, T. Liu, M. Jaroniec and J. Yu, *Mater. Today*, 2019, **25**, 35–65.
119 N. Choudhary, C. Li, J. Moore, N. Nagaiah, L. Zhai, Y. Jung and J. Thomas, *Adv. Mater.*, 2017, **29**, 1605336.
120 F. Béguin, V. Presser, A. Balducci and E. Frackowiak, *Adv. Mater.*, 2014, **26**, 2283.
121 W. W. Zhao, J. L. Peng, W. K. Wang, B. B. Jin, T. T. Chen, S. J. Liu, Q. Zhao and W. Huang, *Small*, 2019, **15**, 1901351.
122 F. F. Cao, M. T. Zhao, Y. F. Yu, B. Chen, Y. Huang, J. Yang, X. H. Cao, Q. P. Lu, X. Zhang, Z. C. Zhang, C. L. Tan and H. Zhang, *J. Am. Chem. Soc.*, 2016, **138**, 6924–6927.
123 P. Zhang, M. Wang, Y. Liu, S. Yang, F. Wang, Y. Li, G. Chen, Z. Li, G. Wang, M. Zhu, R. Dong, M. Yu, O. G. Schmidt and X. Feng, *J. Am. Chem. Soc.*, 2021, **143**, 10168–10176.
124 A. Amiri, A. Bruno and A. A. Polycarpou, *Carbon Energy*, 2023, **5**, e320.
125 G. Pacchioni, *Nat. Rev. Mater.*, 2022, **7**, 844.
126 S. S. K. Mallineni, Y. Dong, H. Behlow, A. M. Rao and R. Podila, *Adv. Energy Mater.*, 2018, **8**, 1702736.
127 Y. Yu, Q. Gao, X. Zhang, D. Zhao, X. Xia, J. Wang, H. Li, Z. L. Wang and T. Cheng, *Energy Environ. Sci.*, 2023, **16**, 3932–3941.
128 Y. Song, N. Wang, Y. Wang, R. Zhang, H. Olin and Y. Yang, *Adv. Energy Mater.*, 2020, **10**, 2002756.
129 G. Conta, A. Libanori, T. Tat, G. Chen and J. Chen, *Adv. Mater.*, 2021, **33**, 2170201.
130 J. Zhang, C. Ye, Y. Liao, C. Sun, Y. Zeng, J. Xiao, Z. Chen, W. Liu, X. Yang and P. Gao, *Mater. Futures*, 2023, **2**, 035101.
131 D.-H. Yang, Z.-Q. Yao, D. Wu, Y.-H. Zhang, Z. Zhou and X.-H. Bu, *J. Mater. Chem. A*, 2016, **4**, 18621–18627.
132 S. Haldar, K. Roy, S. Nandi, D. Chakraborty, D. Puthusseri, Y. Gawli, S. Ogale and R. Vaidhyanathan, *Adv. Energy Mater.*, 2018, **8**, 1702170.
133 S. Gu, S. Wu, L. Cao, M. Li, N. Qin, J. Zhu, Z. Wang, Y. Li, Z. Li, J. Chen and Z. Lu, *J. Am. Chem. Soc.*, 2019, **141**, 9623–9628.

 This journal is © The Royal Society of Chemistry 2024

Published on 10 June 2024. Downloaded by Zhejiang University on 6/25/2024 1:59:47 AM.

134 J. Wang, H. Jia, Z. Liu, J. Yu, L. Cheng, H.-G. Wang, F. Cui and G. Zhu, *Adv. Mater.*, 2024, **36**, 2305605.
135 M. Yang, X. Zeng, M. Xie, Y. Wang, J.-M. Xiao, R.-H. Chen, Z.-J. Yi, Y.-F. Huang, D.-S. Bin and D. Li, *J. Am. Chem. Soc.*, 2024, **146**, 6753–6762.
136 X.-X. Wang, D.-H. Guan, C.-L. Miao, J.-X. Li, J.-Y. Li, X.-Y. Yuan, X.-Y. Ma and J.-J. Xu, *Adv. Energy Mater.*, 2024, **14**, 2303829.
137 Q. Lv, Z. Zhu, Y. Ni, J. Geng and F. Li, *Angew. Chem., Int. Ed.*, 2022, **61**, e202114293.
138 Q. Deng, Y. Yang, W. Zhao, Z. Tang, K. Yin, Y. Song and Y. Zhang, *J. Colloid Interface Sci.*, 2023, **651**, 883–893.
139 J. Han, H. Wu, R. Song, W. Mao, D. Wang and D. Liu, *Electrochim. Acta*, 2024, **477**, 143779.
140 H. Zong, W. Liu, M. Li, S. Gong, K. Yu and Z. Zhu, *ACS Appl. Mater. Interfaces*, 2022, **14**, 10738–10746.
141 C. R. DeBlase, K. E. Silberstein, T.-T. Truong, H. D. Abruña and W. R. Dichtel, *J. Am. Chem. Soc.*, 2013, **135**, 16821–16824.
142 T. Li, X. Yan, Y. Liu, W.-D. Zhang, Q.-T. Fu, H. Zhu, Z. Li and Z.-G. Gu, *Polym. Chem.*, 2020, **11**, 47–52.
143 L. P. Zhai, S. W. Cui, B. L. Tong, W. Chen, Z. J. Wu, C. Soutis, D. Jiang, G. Zhu and L. W. Mi, *Chem. – Eur. J.*, 2020, **26**, 5784–5788.
144 L. P. Zhai, W. T. Wei, B. L. Ma, W. Ye, J. Wang, W. Chen, X. Yang, S. W. Cui, Z. J. Wu, C. Soutis, G. Zhu and L. W. Mi, *ACS Mater. Lett.*, 2020, **2**, 1691–1697.